Cerebellar Nuclei and the Inferior Olivary Nuclei: Organization and Connections

19

Jan Voogd, Yoshikazu Shinoda, Tom J. H. Ruigrok, and Izumi Sugihara

Abstract

The cerebellar nuclei, together with certain vestibular nuclei, are the target of the axons of the Purkinje cells of the cerebellar cortex. Each of these nuclei receives a projection from a longitudinal Purkinje cell zone. Climbing fiber projections are organized according to the same zonal pattern. In this chapter, we will review the morphology and the circuitry of the cerebellar nuclei and the inferior olive and the recurrent pathways connecting them.

Introduction

The cerebellar nuclei, together with certain vestibular nuclei, are the target of the axons of the Purkinje cells of the cerebellar cortex. The projections of the cerebellar nuclei to the brain stem and the distribution of the cerebello-thalamo-cortical paths determine the sphere of influence of the cerebellum. Jansen and Brodal (1940, 1942) were the first to notice that the topographical organization of the Purkinje cell

J. Voogd (✉)
Department of Neuroscience, Erasmus Medical Center Rotterdam, P.O. Box 2040, Rotterdam, 3000 CA, The Netherlands
and
Rhijngeesterstraatweg 1, 2342 AN Oegstgeest, The Netherlands
e-mail: janvoogd@bart.nl

Y. Shinoda • I. Sugihara
Department of Systems Neurophysiology, Graduate School of Medicine, Tokyo Medical and Dental University, 1-5-45 Yushima, Bunkyo-ku, Tokyo, 113-8519, Japan
e-mail: yshinoda.phy1@tmd.ac.jp, isugihara.phy1@tmd.ac.jp

T.J.H. Ruigrok
Department of Neuroscience, Erasmus Medical Center Rotterdam, P.O. Box 2040, Rotterdam, 3000 CA, The Netherlands
e-mail: t.ruigrok@erasmusmc.nl

M. Manto, D.L. Gruol, J.D. Schmahmann, N. Koibuchi, F. Rossi (eds.),
Handbook of the Cerebellum and Cerebellar Disorders,
DOI 10.1007/978-94-007-1333-8_19, © Springer Science+Business Media Dordrecht 2013

projections to the cerebellar nuclei and the olivocerebellar climbing fiber system is very similar. Marr (1969) formulated this similarity in his learning theory of the cerebellar cortex as "the olivary cell should respond to a command for the same elemental movement as is initiated by the corresponding Purkinje cell." In this chapter, we will review the morphology of the cerebellar nuclei and the inferior olive, the afferent connections of the olive, the zonal organization of the corticonuclear and olivocerebellar projection, and the efferent connections of the cerebellar nuclei and the presence of recurrent cerebellar-brain stem circuitry.

The Cerebellar Nuclei

Four cerebellar nuclei, known as the fastigial emboliform, globose, and dentate nucleus, were distinguished in the human cerebellum by Stilling (1864). The same four nuclei can be distinguished in different mammalian species, where they are known as the medial, anterior interposed, posterior interposed, and lateral cerebellar nucleus (Ogawa 1935; Weidenreich 1899) (Fig. 19.1). The cerebellar nuclei are arranged in two groups. The rostrolateral group consists of the anterior interposed nucleus (emboliform) that is connected with the lateral (dentate) nucleus. The caudomedial group consists of the medial (fastigial) nucleus with the posterior interposed (globose) nucleus. A fifth cerebellar nucleus, located at the border of the fastigial and posterior interposed nucleus, known as the "interstitial cell groups" was distinguished by Buisseret-Delmas and Angaut (1993) in the rat but appears to be present in other mammals (Fig. 19.1a, b).

Three populations of neurons have been distinguished in all cerebellar nuclei. The main population consists of excitatory relay cells with widespread, branching axons, terminating in the brain stem, the spinal cord, and the thalamus. They constitute a mixed population of cells of all shapes and sizes (Courville and Cooper 1970). Most relay cells of the cerebellar nuclei are glutamatergic. Large, glycinergic neurons that give rise to the ipsilateral projections of the fastigial nucleus were identified in mice (Bagnall et al. 2009). Small GABAergic neurons, that project exclusively to the inferior olive constitute a second population, present in all nuclei (Graybiel et al. 1973; Mugnaini and Oertel 1985) (see also section "The Nucleo-olivary Pathway"). A third population of small interneurons was identified by Chan-Palay (1977) on morphological grounds in the monkey, by Chen and Hillman (1993) as glycinergic neurons, and by Leto et al. (2006) as GABAergic neurons, all in rodents. Glycinergic neurons, with projections to the cerebellar cortex, were described in the mouse lateral cerebellar nucleus (Uusisaari and Knopfel 2010). Before, all recurrent projections from the cerebellar nuclei to the cortex were supposed to originate as collaterals from the relay cells (McCrea et al. 1978).

The fastigial nucleus is located next to the midline. In rodents, a prominent protrusion, known as the dorsolateral protuberance (Goodman et al. 1963), is present that is lacking in carnivores and primates (Fig. 19.1a). The rodent anterior interposed nucleus includes a lateral portion, indicated as the dorsolateral hump that

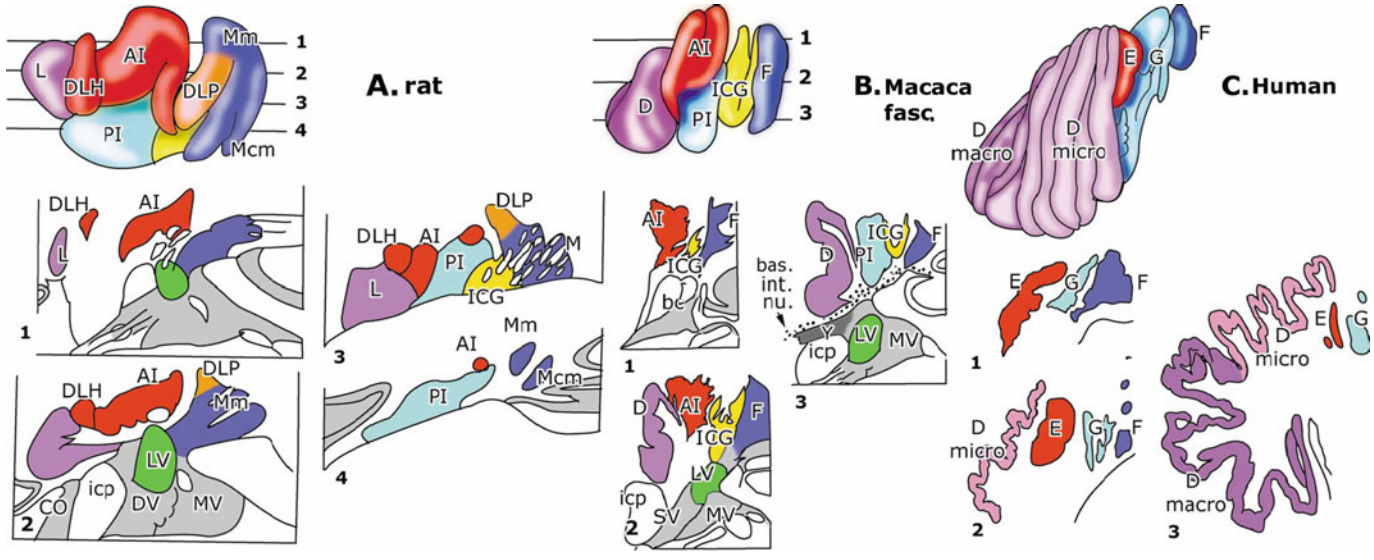

Fig. 19.1 The cerebellar nuclei of the rat, *Macaca fascicularis*, and the human cerebellum: dorsal aspect and selected transverse sections. Abbreviations: *AI* anterior interposed nucleus, *bc* brachium conjunctivum, *CO* cochlear nucleus, *D micro* microgyric part of the dentate nucleus, *D* dentate nucleus, *DLH* dorsolateral hump, *DLP* dorsolateral protuberance, *D macro* macrogyric part of the dentate nucleus, *DV* descending vestibular nucleus, *E* emboliform nucleus, *F* fastigial nucleus, *G* globose nucleus, *ICG* interstitial cell groups, *icp* inferior cerebellar peduncle, *int.nu.* basal interstitial nucleus, *L* lateral cerebellar nucleus, *LV* lateral vestibular nucleus, *Mcm* caudomedial subdivision of the medial nucleus, *Mn* medial subdivision of the medial nucleus, *MV* medial vestibular nucleus, *PI* posterior interposed nucleus, *SV* superior vestibular nucleus, *Y* group Y

sometimes is allocated to the lateral cerebellar nucleus. A parvocellular subnucleus occupies the ventral part of the lateral cerebellar nucleus in these species.

The primate dentate nucleus has the shape of a "crumpled purse" (Chan-Palay 1977) with its hilus directed ventromedially and rostrally. In the human cerebellum, two parts of the nucleus can be distinguished, a microgyric and a macrogyric portion (Fig. 19.1c). The dorsomedial, microgyric portion is folded in rather narrow, rostrocaudally directed ridges. The ridges in the ventrolateral, macrogyric portion of the nucleus are broad and subdivided, and the cell band in this part of the nucleus is wider than in the microgyric part. The cells of the microgyric part of the dentate are larger than those in the macrogyric position of the nucleus (Demolé 1927a, b), but both subdivisions also contain small neurons. This subdivision had already been noticed by Vicq d'Azyr in the first accurate description of the nucleus lateral, dating from the eighteenth century (Glickstein et al. 2009). The ontogenetic development of the macrogyric portion lags far behind the microgyric (Weidenreich 1899). Unfortunately, there are no indications how the two parts of the human dentate are represented in the monkey dentate.

A prominent Y nucleus is present, ventral to the dentate, in the monkey cerebellum (Fig. 19.1b). It should be distinguished from Ill-defined groups of small acetylcholinesterase-positive cells dispersed in the white matter of the flocculus and the nodule and ventral to the dentate and the posterior interposed nucleus, in the roof of the fourth ventricle known as the basal interstitial nucleus (Fig. 19.1b). The basal interstitial nucleus is reciprocally connected with the flocculus (Langer et al. 1985) and, possibly, with the nodulus. The group Y is a lateral extension of the superior vestibular nucleus that gives rise to projections to the oculomotor nuclei (Graybiel and Hartwieg 1974; Stanton 1980a; Steiger and Büttner-Ennever 1979; Yamamoto et al. 1986). Langer's basal interstitial nucleus and the group Y are well-defined nuclei in the monkey cerebellum but have not yet been recognized in the human cerebellum.

Subdivision of the Inferior Olive

The inferior olive derives its name from the olive-shaped prominence on the ventrolateral surface of the medulla. The first description of the nuclei of the inferior olive dates from Stilling (1843). He identified the principal olive, the medial accessory olive (as the "grossen Pyramidenkern") and the dorsal accessory olive (his "Oliven Nebenkern") in sections through the human medulla oblongata. Sections through the inferior olive of the human brain and of different species that have been used in experimental studies of the connections of the inferior olive are illustrated in Figs. 19.2 and 19.3. Diagrams of surface-projections of the olivary nuclei, first constructed by Brodal (1940) showing the position of the sections, are included in these figures. Subdivisions of the principal and the accessory olives have been distinguished by inspection of the shape and contour of these nuclei, but their definite identification depends on the recognition of their connections. Moreover, species-specific subdivisions may occur.

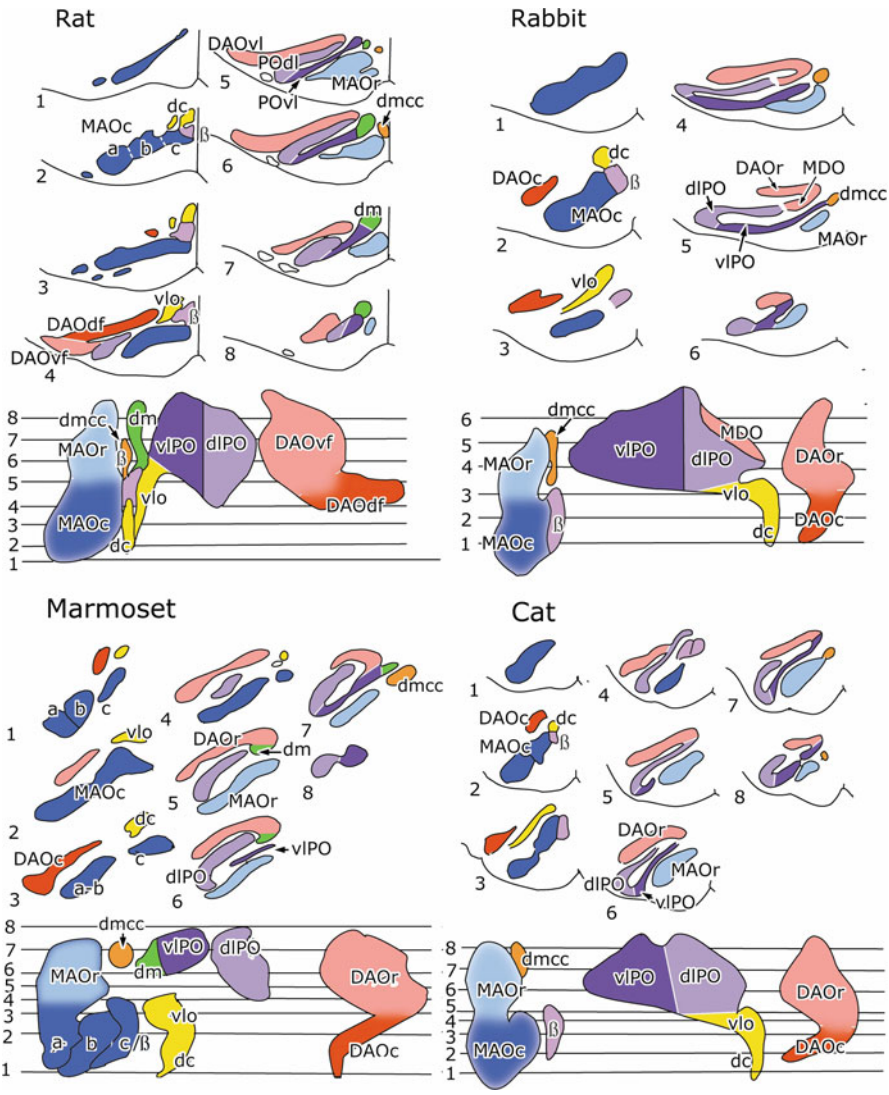

Fig. 19.2 Diagrams of selected transverse sections through the inferior olive and surface-projections of its subnuclei of different mammalian species (Redrawn from Brodal (1940), rabbit and cat; Ruigrok and Voogd (1990), rat; and Fujita et al. (2010), marmoset). Abbreviations: *a*, *b*, *c* subnuclei a, b, c of the caudal medial accessory olive, *ß* group beta, *DAOc* caudal dorsal accessory olive, *DAOdf* dorsal fold of the dorsal accessory olive, *DAOr* rostral dorsal accessory olive, *DAOvf* ventral fold of the dorsal accessory olive, *dlPO* dorsal lamina of the principal olive, *dm* dorsomedial group, *dmcc* dorsomedial cell column, *MAOc* caudal medial accessory olive, *MAOr* rostral medial accessory olive, *MDO* medial part dorsal accessory olive, *vlo* ventrolateral outgrowth, *vlPO* ventral lamina of the principal olive

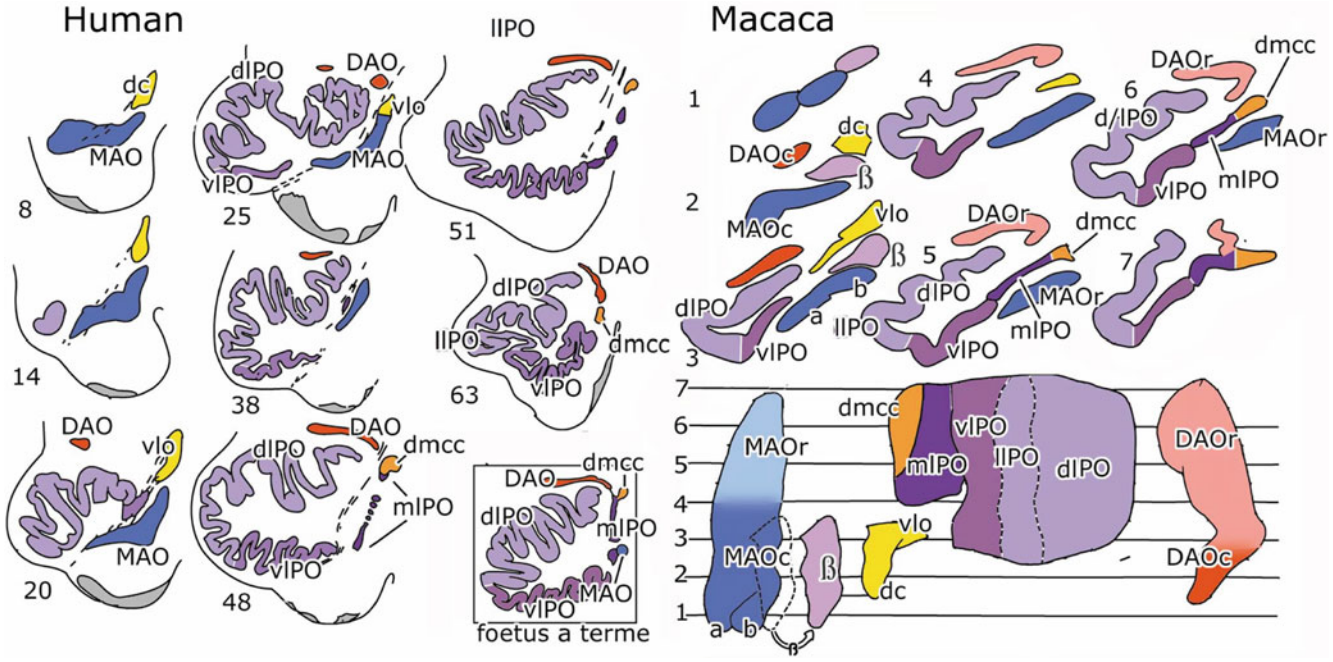

Fig. 19.3 Diagrams of selected transverse sections through the human inferior olive and of transverse sections and a surface projection of its subnuclei of the macaque monkey (Human inferior olive redrawn from Marechal (1934)). Abbreviations: *llPO* lateral lamina of the principal olive, *mlPO* medial lamina of the principal olive. For other abbreviations, see Fig. 19.2

The medial accessory olive can be subdivided into caudal (MAOc) and rostral (MAOr) parts. The MAOc often has been further subdivided into the mediolaterally disposed subgroups a, b, and c. (Fig. 19.1, rat section 2, marmoset, sections 1–3; Fig. 19.2, macaque monkey, section 3). This subdivision is not distinct at all levels. Moreover, in the rat, subgroups a–c were distinguished, in addition to the group beta, which forms a fourth, medial subdivision of the MAOc, whereas in the macaque monkey, subgroup c is identical to the group beta. The group beta was first distinguished by Brodal (1940). In the cat and the rabbit, it is aligned with the more rostrally located dorsomedial cell column (DMCC).

The DMCC was first distinguished by Bertrand and Marechal (1930) in the human inferior olive as a rostrally located cell group, attached to the medial pole of the DAO and, ventrally, to the medial lamella of the principal olive (Fig. 19.3, section 48). This position is even more distinct at late fetal stages (Fig. 19.3, inset). In the cat and the rabbit, Brodal (1940) identified a cell group with a different position, located dorsomedial to the rostral MAO, as the DMCC (Fig. 19.2). In the rat, Brodal's DMCC is present, but it should be distinguished from another subgroup, the dorsomedial group (Azizi and Woodward 1987). The dorsomedial group in the rat is attached to the medial pole of the ventral lamina of the principal olive, a position it shares with the DMCC from Marechal's original description. In macaque monkeys, the cell group identified as the DMCC is attached to the medial lamella of the PO and/or the medial pole of the DAO and, therefore, occupies the same position as the human DMCC and the rat dorsomedial group (Bowman and Sladek 1973; Brodal and Brodal 1981; Whitworth and Haines 1986a, b) (Figs. 19.2 and 19.3). In the marmoset, both cell groups can be distinguished (Fujita et al. 2010). The connections of the two cell groups are different: the DMCC as present in cat, rabbit, and rat receives vestibular input, the dorsomedial group and the monkey DMCC (Fig. 19.3, right panel, sections 5,6), are innervated by somatosensory systems. A cell group corresponding to the cat DMCC, innervated by the vestibular system, has not been identified in monkeys.

At the level of the MAOc, the dorsal cap (DC) of Kooy (1917) is located dorsal to the group beta. More rostrally, it extends medially as the ventrolateral outgrowth (VLO).

The dorsal accessory olive can be divided into caudal (DAOc) and rostral (DAOr) parts. In the rat, the DAOc is folded over the DAOr, and the two divisions of the DAO are known as the dorsal and ventral fold of the DAO (Azizi and Woodward 1987). In surface projections, the DAOc typically forms a caudomedially directed extension of the DAO.

The principal olive generally is subdivided into dorsal (dlPO) and ventral (vlPO) laminae. In rat, cat, rabbit, and marmoset, the cell band of the vlPO is thinner than the broad cell band of the dlPO. At some levels, a gap or a constriction separates the vlPO from the dlPO in rat and cat. In artiodactyles, the ventral lamina is always separated from the rest of the PO (Whitworth and Haines 1986b). In the macaque monkey, an additional lateral lamina or "bend" was distinguished. In monkeys, the great apes and in the human inferior olive the dorsal (dlPO), lateral (llPO) and the lateral portion of the ventral lamina, indicated as the vlPO, display the typical convolutions of the inferior olive. In monkeys, the thin, nonvoluted portion of the

vlPO is indicted as the mlPO (Fig. 19.3). In the human inferior olive, Kooy (1917) and Bertrand and Marechal (1930) described a narrow, medial lamina (mlPO), located medial to the MAO (Fig. 19.3, sections 38–51).

In rabbit and rat, the medial pole of the DAOr is connected with the dlPO. In the cat and the marmoset, a similar connection exists with the vlPO. In the human and macaque inferior, the DAOr and the laminae of the principal olive remain isolated from each other. The VLO is continuous with the vlPO in the rat and in the human inferior olive and with the dlPO in the rabbit and the cat. No such continuity appears to exist in the marmoset and the macaque monkey.

Afferent Connections of the Inferior Olive

Four main categories of afferents of the inferior olive, each with their own distribution, can be distinguished. The inferior olive processes somatosensory input mostly in the MAOc and DAO, vestibular and optokinetic input in the DC/VLO/ group beta, visual information in the medial part of MAOc. The PO and MAOr process information relayed by nuclei at the mesodiencephalic border from the cerebral cortex. However, overlap between the various modalities within olivary subnuclei has been noted. Below, we provide a more detailed account of these projections.

Projections from Spinal Cord, Trigeminal Nuclei, and Dorsal Column Nuclei

Ventral Spino-olivary Pathways

Spino-olivary fibers originate mainly from the contralateral cervical and lumbar gray matter, ascend in the ventral funiculus, and terminate in the caudal MAOc and, laterally, in caudal and rostral parts of the DAO (Fig. 19.4) (Boesten and Voogd 1975; Armstrong and Schild 1979; Armstrong et al. 1982). The system has been described in different mammalian species, but not in monkeys (Brodal et al. 1950; Brown et al. 1977; Martin et al. 1980; Mizuno 1966; Swenson and Castro 1983a, b; Whitworth and Haines 1983). Detailed information on the anatomy and the physiology of the ventral funiculus olivocerebellar pathway (vfSOCP) (Oscarsson and Sjölund 1977a, b, c) is available for the cat (Fig. 19.22a). Spino-olivary fibers originate from the medial ventral horn (Rexed's (1952) lamina VIII), the nucleus proprius of the dorsal horn (laminae IV/V), cells in the lateral funiculus and the intermediate gray (lamina VII). Except for lower cervical levels, all neurons giving rise to spino-olivary fibers are located contralaterally. The majority of the system takes its origin from the lumbar and sacral cord, the contribution of the thoracic cord is negligible and of the cervical cord rather small. The lateral cervical nucleus does not contribute to the projection (Armstrong and Schild 1979; Armstrong et al. 1982; Buisseret-Delmas 1982; Molinari 1984, 1985; Richmond et al. 1982).

Lumbar and sacral spino-olivary fibers terminate ventrolaterally in the MAOc, overlapping with the projection from the cervical cord that extends more medially.

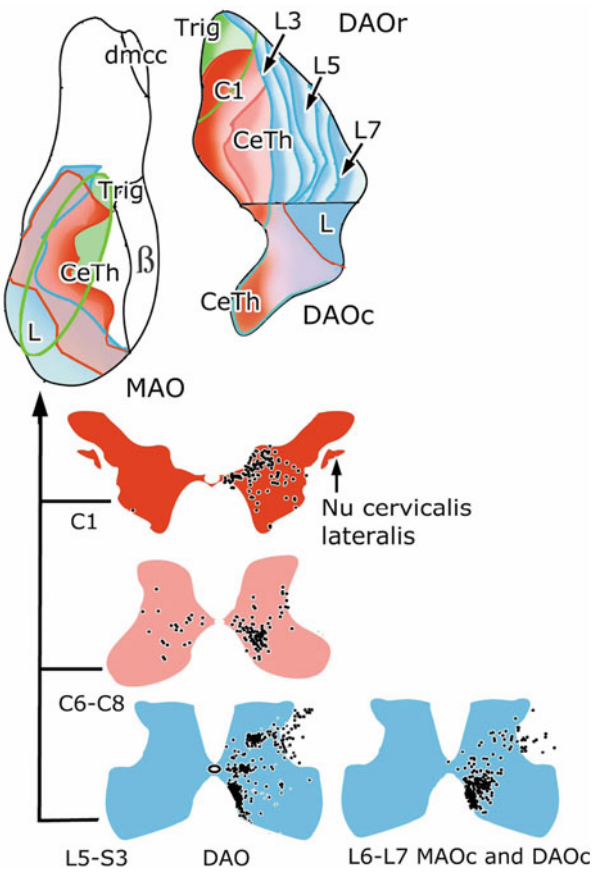

Fig. 19.4 The ventral funiculus spino-olivary pathway in the cat. The origin of this system is illustrated in diagrams of the lumbosacral cord for cells retrogradely labeled from the entire DAO (L5-S3, Molinari 1984) and from the caudal MAO and DAO (L6-L7, Molinari 1985), the low cervical (Armstrong et al. 1982), and high cervical cord (Richmond et al. 1982). Projections from these levels to the contralateral MAOc and DAOc show much overlap, and a more distinct topical projection is present in the DAOr (Armstrong et al. 1982; Boesten and Voogd 1975). A projection from the contralateral spinal trigeminal nucleus (Trig) occupies the rostromedial MAOc and the medial DAOr (Courville et al. 1983b) (Redrawn from illustrations of the cited papers). For abbreviations, see Fig. 19.1

A similar overlap of sacrolumbar and cervical afferents is present in the caudal DAO. In the rostral DAO, a distinct somatotopical organization is present, with lumbar and cervical fibers terminating in increasingly more medially located lamellae (Armstrong et al. 1982; Boesten and Voogd 1975; Richmond et al. 1982). A very similar somatotopical organization was found in the DAO of the cat for the distribution of evoked potentials on peripheral stimulation (Fig. 19.5) (Gellman et al. 1983). Evoked potentials from light cutaneous stimuli predominate over deep input from muscles and fascia in DAOr, and the latter predominate in the DAOc. These recordings represent the combined projections from the ventral and the dorsal column spino-olivary pathways.

Projections to the MAOc and the DAOc originate mainly from the medial ventral horn and projections to the DAOr from the dorsal horn. The intermediate gray projects to both accessory olives (Molinari 1984, 1985). Spino-olivary fibers terminate as boutons containing spherical vesicles, with asymmetrical synapses on dendritic shafts and spines, more inside than outside the glomeruli (King et al. 1975; Molinari and Starr 1989).

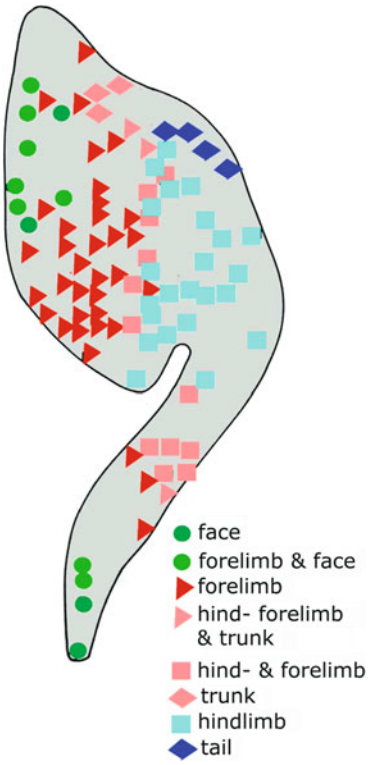

Fig. 19.5 Somatotopical localization in the dorsal accessory olive of the cat (Redrawn from Gellman et al. (1983))

Projections from the Sensory Nuclei of the Trigeminal Nerve

The sensory trigeminal nuclei project to the extreme medial part of the contralateral DAOr (Cook and Wiesendanger 1976) and, in addition, to the adjoining vlPO in the cat and the rabbit (Van Ham and Yeo 1992), to the dorsomedial group in the rat (Huerta et al. 1983) and to a separate region in the vlPO in the rabbit (Van Ham and Yeo 1992). No terminations are present in the dorsomedial cell column in any of these species (Fig. 19.6). In the MAOc, the trigeminal nuclei project to its rostromedial region, next to the rostral pole of the group beta in all species where they overlap with the terminals from the cuneate nucleus (see section "Projections from the Dorsal Column Nuclei" and Fig. 19.6c). In the cat, the projection extends more caudally, overlapping with the terminals from the cervical cord (Fig. 19.6). Interestingly, terminations in the rat DAOr were identified as collateral projections of the trigemino-tectal pathway, but the projection of the trigeminal nuclei to the MAOc is an unbranched system (Huerta et al. 1983). No data on the trigemino-olivary projection are available for primates. Most authors agree that the main origin of the trigemino-olivary projection is located in the pars interpolaris of the spinal nucleus (Huerta et al. 1983; Huerta and Harting 1984; Swenson and Castro 1983a; Van Ham and Yeo 1992; Walberg 1982), although some also include the principal sensory nucleus and the pars caudalis.

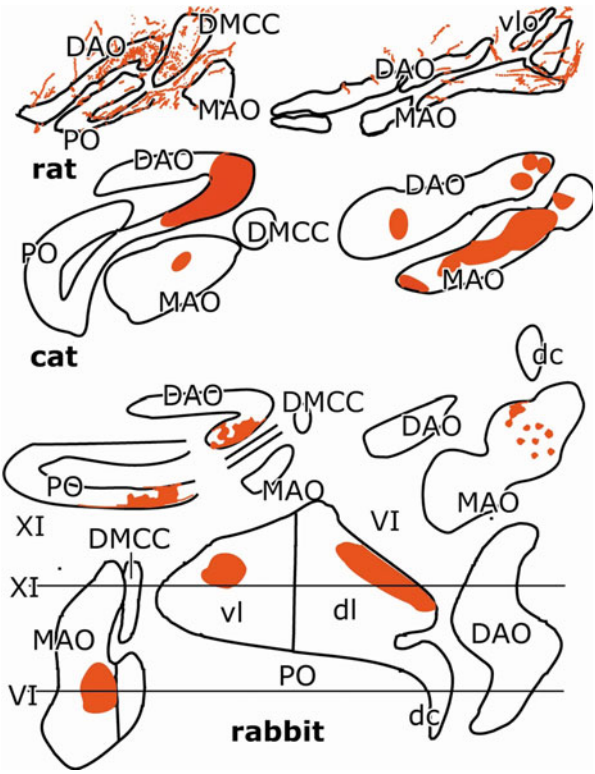

Fig. 19.6 Localization of projections of the contralateral spinal trigeminal nucleus illustrated in a rostral and a more caudal section through the inferior olive of the rat (Huerta et al. 1983), the cat (Berkley and Hand 1978), and in transverse sections and a diagram of the flattened inferior olive of the rabbit (Van Ham and Yeo 1992). For abbreviations, see Fig. 19.2

Projections from the Dorsal Column Nuclei

Two fiber systems occupy the dorsal columns: the ascending branches of the dorsal root fibers and the postsynaptic dorsal column pathway that contains an extra synapse in the dorsal horn (Fig. 19.7). Both pathways transmit somatosensory information to the dorsal column nuclei, but the latter pathway has been shown to be responsible for the transmission of nociceptive input to the inferior olive in the cat (Ekerot et al. 1991). The connectivity in the dorsal funiculus spino-olivocerebellar pathway (df-SOCP) has been extensively studied by Ekerot and Larson (1979a, b) (Fig. 19.22b). In the dorsal column nuclei of the cat, the fusiform cells that project to the contralateral inferior olive are located outside the cell cluster regions of the internal and gracile nuclei, which give rise to the medial lemniscus (Fig. 19.8). Neurons of the gracile nucleus that project to the rostral and caudal DAO accumulate rostral to the cluster region in the transitional portion of the nucleus. The main projection is to the DAOr. The numbers of the cells labeled from injections of retrograde tracers in the DAOc and the MAOc are small (Molinari 1984, 1985). A wider distribution of neurons with projections to the inferior olive was found for the internal cuneate nucleus (Alonso et al. 1986; Buisseret-Delmas 1982) (Fig. 19.8).

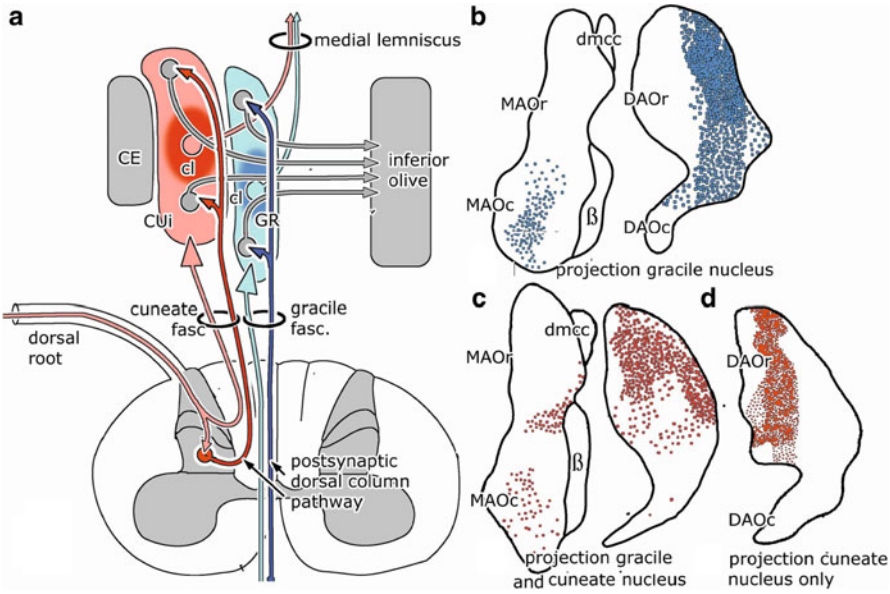

Fig. 19.7 The dorsal funiculus spino-olivary pathway in the cat. (**a**) Both ascending collaterals from spinal root fibers and the postsynaptic dorsal column pathway partcipate in the projection to the dorsal column nuclei. Projections to the inferior olive take their origin from regions outside the cell clusters (cl) that give origin to the medial lemniscus. (**b**) Projections from the contralateral gracile nucleus (Boesten and Voogd 1975). (**c**) Projections from the contralateral gracile and internal cuneate nuclei (Boesten and Voogd 1975). (**d**) Projections from the contralateral cuneate nucleus (Groenewegen et al. 1975) (**b–d** redrawn from illustrations of the cited papers). Abbreviations: *CE* external cuneate nucleus, *Cui*, internal cuneate nucleus, *GR* gracile nucleus. For other abbreviations, see Fig. 19.2

The projections from the gracile and internal cuneate nuclei occupy lateral and more medial bands in the DAOr and mostly spare the DAOc (Fig. 19.7b, d). A minor projection from the gracile nucleus is present in the MAOc (Figs. 19.7b and 19.8). Terminals from the internal cuneate nucleus are found in the rostromedial MAOc at its border with the MAOr (Fig. 19.7c), a region that also receives a projection from the spinal trigeminal nucleus (Fig. 19.5). Projections to the ipsilateral inferior olive from the dorsal column nuclei, described by several authors, may originate from the adjoining reticular formation (Courville et al. 1983b).

Few data are available for the projection of the dorsal column nuclei to the inferior olive in monkeys. Sections of cases from Kalil (1979) and Molinari et al. (1996), illustrated in Fig. 19.9, show terminations in the DAOr, the DMCC, and the rostromedial MAOc. These projections are in accordance with the findings in cats, with the exception of the DMCC that receives vestibular, rather than somatosensory input in this species. It may be that the monkey DMCC corresponds to the dorsomedial group, as identified in the rat, rather than with the DMCC of other species.

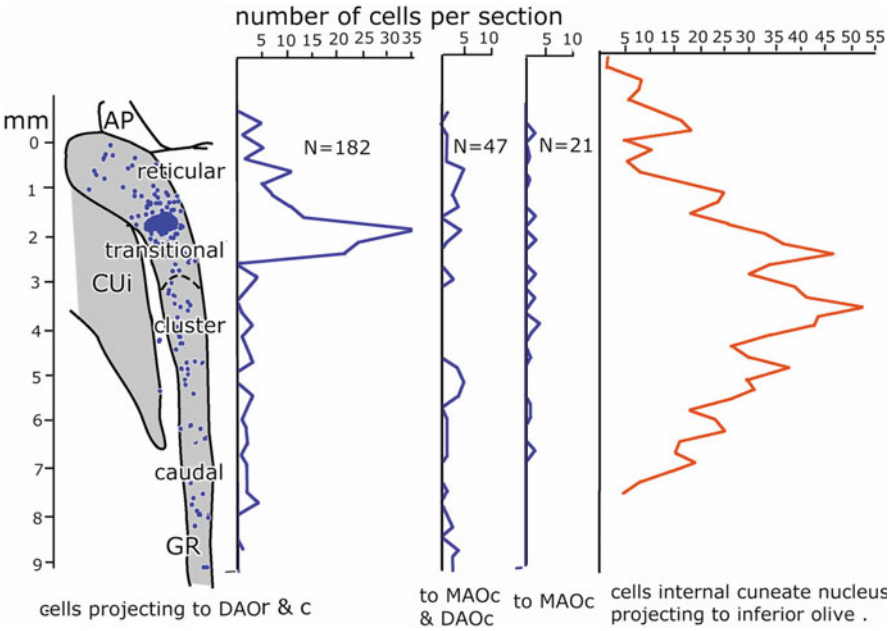

Fig. 19.8 Localization of neurons of the dorsal column nuclei projecting to the contralateral inferior olive in the cat. *Left panels* (*blue*) show the location of neurons in the gracile nucleus and the rostrocaudal distribution of neurons projecting to the entire DAO, the MAOc and the DAOc and the MAOc only (Molinari 1984, 1985). *Right panel* shows the distribution of neurons of the internal cuneate nucleus after large injections of a retrograde tracer in the inferior olive (Alonso et al. 1986) (Redrawn from illustrations of the cited papers). Abbreviations: *AP* area postrema, *Cui* internal cuneate nucleus, *GR* gracile nucleus

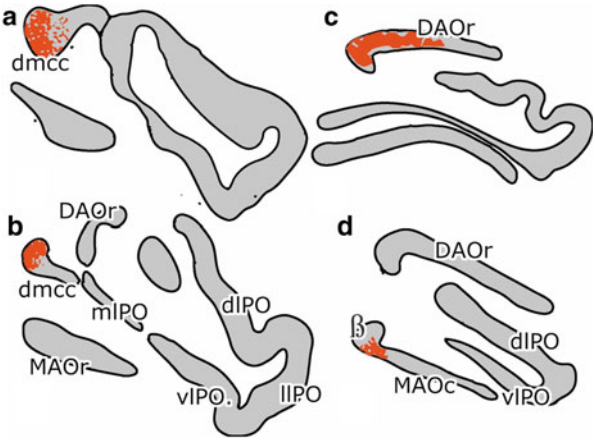

Fig. 19.9 Projections from the internal cuneate nucleus of the macaque monkey. (**a**) is the most rostral section (**a** and **d** redrawn from Kalil (1979), **c** and **d** from Molinari et al. (1996)). Abbreviations see Fig. 19.2

Electron microscopic studies of the dorsal column-olivary projection documented its terminals as excitatory boutons with spherical vesicles and asymmetrical synaptic contacts (Molinari et al. 1991). GABAergic neurons in the cuneate and less in the gracile nucleus, with projections to the contralateral inferior olive, were observed by Nelson and Mugnaini in the rat (1989).

Alternative routes for the transmission of peripheral input to the inferior olive are provided by ascending spinal, trigeminal, and dorsal column pathways terminating in the pretectum that innervates the DAOr (see below), in Darkschewitsch nucleus that innervates the DAOr, or in the parvocellular red nucleus that innervates the principal olive (Wiberg and Blomqvist 1984a, b; Wiberg et al. 1986, 1987).

Optokinetic and Vestibular Projections to the Inferior Olive

The optokinetic system with its projections of the nuclei of the accessory optic system and the nucleus of the optic tract in the mesencephalon to the dorsal cap (DC) and the ventrolateral outgrowth (VLO) recently was reviewed by Giolli et al. (2006), Barmack (2006), and Voogd (Voogd and Barmack 2006; Voogd et al. 2011). For complete references, we refer to these reviews. DC and VLO receive information on global movements of the visual surround from large field ganglion cells in the contralateral retina via the optic tract (Fig. 19.10a). These movements generate retinal slip signals, which can serve as an error signal in long-term adaptation of the vestibulo-ocular and optokinetic reflexes. The retinal slip signals around a vertical axis excite neurons of the nucleus of the optic tract and the dorsal nucleus of the accessory system. These nuclei project to the DC of the ipsilateral inferior olive. Global movements of the visual surround around an oblique horizontal axis at 45° azimuth, that is approximately colinear with the axis of the ipsilateral anterior semicircular canal, are transmitted bilaterally by the medial and lateral nuclei of the accessory optic system and contralaterally by the visual tegmental relay zone. These nuclei project to the VLO. The organization of the accessory optic system and the projections of its subnuclei to the inferior olive in primates is very similar to that in lower mammals. The border between the projections of vertical axis and horizontal axis neurons in the rabbit is located halfway within the dorsal cap. Consequently, the two functional subdivisions in this species correspond to the VLO and the rostral dorsal cap that relay information from horizontal axis neurons, and the caudal dorsal cap that serves as the relay for the vertical axis neurons. The VLO merges with the vlPO, and the vertical axis subdivision may spill over in this lamina in species like the rat.

The DC and the VLO receive additional input from the paramedian reticular formation (Fig. 19.10b), the dorsal group Y, and the nucleus prepositus hypoglossi (Fig. 19.11a). The paramedian reticular formation is involved in the generation of saccades. Its projection to the dorsal cap has been identified only in the cat (Gerrits and Voogd 1986). The dorsal group Y is located within the floccular peduncle and is the target of Purkinje cell zones influencing eye movements about a similar horizontal axis as the cells of the VLO. In the cat, it projects to the contralateral VLO

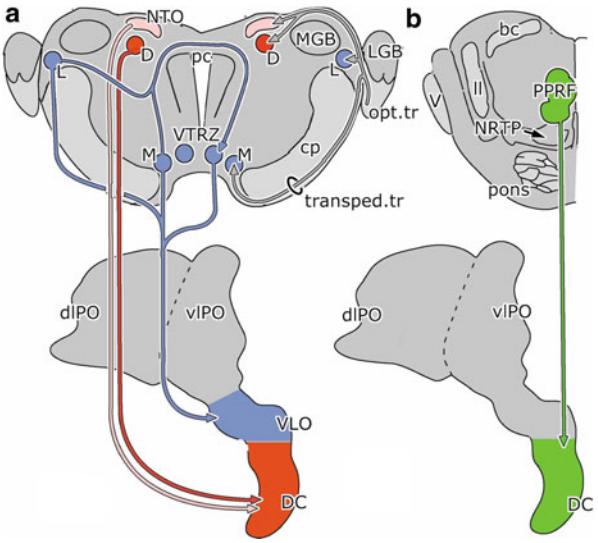

Fig. 19.10 Optokinetic and vestibular afferents of the inferior olive. (**a**) Projection of the nuclei of the accessory optic system and the nucleus of the optic tract on to the dorsal cap and the ventrolateral outgrowth. (**b**) Map of the projection of the paramedian pontine reticular formation to the dorsal cap in the cat (Gerrits and Voogd 1986). Abbreviations: *bc* brachium conjunctivum, *cp* cerebral peduncle, *D* dorsal nucleus of the accessory optic system, *DC* dorsal cap, *dlPO* dorsal lamina of the principal olive, *L* lateral nucleus of the accessory optic system, *LGB* lateral geniculate body, *ll* lateral lemniscus, *M* medial nucleus of the accessory optic system, *MGB* medial geniculate body, *NRTP* nucleus reticularis tegmenti pontis, *NTO* nucleus of the optic tract, *opt.tr* optic tract, *Pc* posterior commissure, *PPRF* paramedian pontine reticular formation, *transped.tr* transpeduncular tract, *V* trigeminal nerve, *VLO* ventrolateral outgrowth, *vlPO* ventral lamina of the principal olive, *VTRZ* ventral tegmental reflex zone

(Gerrits et al. 1985), and in the rabbit, this projection also includes the rostral DC (De Zeeuw et al. 1994a). This projection is GABAergic. The nucleus prepositus hypoglossi has a role in gaze-holding. Separate neuronal populations connect it with the horizontal gaze center in the paramedian reticular formation, the vestibular nuclei, the cerebellum, and the inferior olive (McCrea and Baker 1985). The projection of the nucleus prepositus hypoglossi to the dorsal cap is contralateral in the cat and rat (Barmack et al. 1993; Gerrits et al. 1985), but bilateral in the rabbit (De Zeeuw et al. 1993). This projection consists of a mixture of cholinergic and GABAergic afferents and of elements expressing both transmitters (Barmack et al. 1993; De Zeeuw et al. 1993).

According to Barmack (2006), vestibular input to the group beta and the DMCC is organized as a simple push-pull system, with excitatory input from the group Y and inhibition from the parasolitary nucleus. A projection of the group Y to the contralateral DMCC (but not to the group beta) was traced in the cat (Gerrits et al. 1985) (Fig. 19.11a) but not in the rabbit (De Zeeuw et al. 1994a) where this system, moreover, was found to be GABAergic. The parasolitary nucleus is located lateral to the solitary nucleus, next to the caudal pole of the descending vestibular nucleus

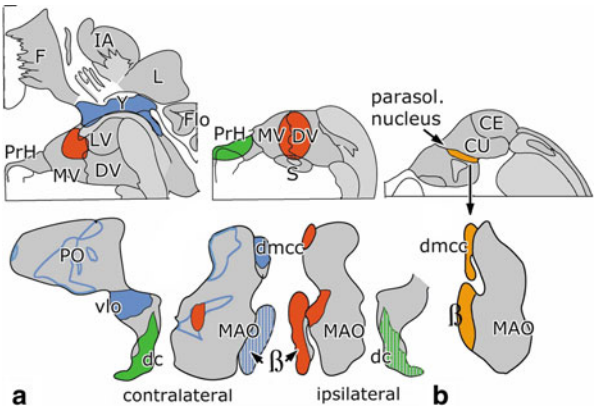

Fig. 19.11 (**a**) Injection sites of antegrade tracers in different parts of the vestibular nuclei, the group Y and the nucleus prepositus hypoglossi and their projections to the inferior olive (Redrawn from Gerrits et al. (1985). Additional projections (of the group Y to the contralateral group beta (Barmack 2006) and of the nucleus prepositus hypoglossi to the ipsilateral dorsal cap (De Zeeuw et al. 1993) are hatched. (**b**) Projection of the parasolitary nucleus to the group beta in the rat (Redrawn from Barmack et al. (1998)). Abbreviations: *F* fastigial nucleus, *IA* anterior interposed nucleus, *L* lateral cerebellar nucleus, *Y* group Y, *FlO* flocculus, *LV* lateral vestibular nucleus, *DV* descending vestibular nucleus, *MV* medial vestibular nucleus, *PrH* nucleus prepositus hypoglossi, *S* nucleus of the solitary tract, *CE* external cuneate nucleus, *CU* internal cuneate nucleus, *PO* principal olive, *vlo* ventrolateral outgrowth, *dc* dorsal cap, *dmcc* dorsomedial cell column, *MAO* medial accessory olive, *ß* group beta

(Fig. 19.11b). It receives root fibers from branches of the vestibular nerve that innervate the ampullae of the vertical canals and the utriculus. Its small, compact neurons provide the ipsilateral group beta and the DMCC with inhibitory synapses (Barmack et al. 1998; Loewy and Burton 1978; Molinari and Starr 1989).

Projections of the medial and descending vestibular nuclei to the ipsilateral group beta and the DMCC were found by several authors in cat, rat, and rabbit (Barmack et al. 1993; Brown et al. 1977; Gerrits et al. 1985; Nelson and Mugnaini 1989; Saint-Cyr and Courville 1979; Swenson and Castro 1983a) (Fig. 19.11a). Signals from the ipsilateral anterior semicircular canals, relayed through the parasolitary nucleus, are mapped upon the caudal group beta, signals from the posterior canal onto its rostral part. There are no projections from the horizontal canal. DMCC neurons respond preferentially to otolithic stimulation. The pattern of vestibularly modulated activity in DMCC neurons is consistent with an inhibitory vestibulo-olivary projection, supposedly from the parasolitary nucleus (Barmack 2006).

Afferents from Tectum and Pretectum

A contralateral projection of the superior colliculus to the medial MAOc, located next to the group beta, was demonstrated in rat, cat, rabbit, and monkey

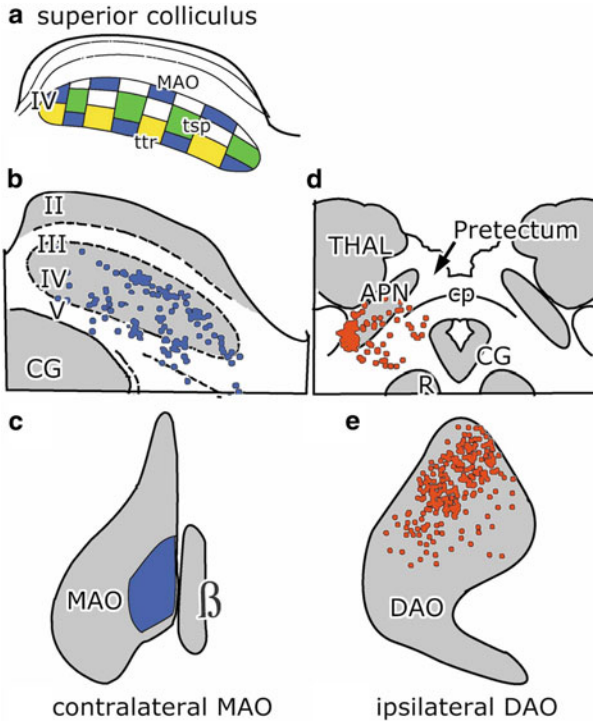

Fig. 19.12 Projections to the inferior olive from the tectum and the pretectum. (**a**–**c**) The tecto-olivary projection. (**a**, **b**) Tecto-olivary neurons in the cat are located in the intermediate gray layer as part of a grid, where they alternate with tectospinal (green) and tectotrigeminal (yellow) neurons (Redrawn from Huerta and Harting (1984) and Weber et al. (1978)). (**c**) Termination in the rat of tecto-olivary projection in medial MAOc (Akaike 1992). (**d**, **e**) The pretecto-olivary projection in the cat. (**d**) Origin from the anterior pretectal nucleus (Kitao et al. 1989). (**e**) Termination in the DAOr (Kawamura and Onodera 1984). Abbreviations: *APN* anterior pretectal nucleus, *CG* central gray, *Cp* posterior commissure, *DAO* dorsal accessory olive, *GC* central gray, *II-V* layers II-V of the superior colliculus, *MAO* medial accessory olive, *MAO* neurons projecting to MAOc, *R* red nucleus, *THAL* thalamus, *tsp* tectospinal neurons, *ttr* tectotrigeminal neurons

(Frankfurter et al. 1976; Harting 1977; Hess and Voogd 1986; Holstege and Collewijn 1982; Saint-Cyr and Courville 1982; Weber et al. 1978) (Fig. 19.12c). It takes its origin from the fourth, intermediate gray lamina of the superior colliculus. When Weber's (Weber et al. 1978) plot of the neurons that were labeled retrogradely from the inferior olive (Fig. 19.12b) is examined, these neurons appear to be located in layers or patches in the superficial and deep parts of the intermediate gray. Huerta and Harting (1984) found similar patches of neurons with projections to the inferior olive to be arranged in a grid in the intermediate gray layer that also contains neurons with projections to the trigeminal nuclei and those giving rise to the predorsal fascicle (Fig. 19.12a). The functional meaning of this organization is not

known. In the rat MAOc, the tecto-olivary projection remains separated from the more laterally and rostrally terminating trigemino-olivary pathway (Akaike 1989).

The ventral anterior pretectal nucleus and scattered neurons in the pretectum, that may belong to the dorsal pretectal nucleus and the nucleus of the posterior commissure, have been found to project to the ipsilateral DAOr in the rabbit and cat (Itoh et al. 1983; Kawamura and Onodera 1984; Kitao et al. 1989) (Fig. 19.12d, e). These nuclei receive afferents from the dorsal column nuclei. In the DAOr, the projections from the pretectum and the dorsal column nuclei overlap (Kawamura et al. 1982; Bull et al. 1990).

Nuclei at the Mesodiencephalic Border: The Central and Medial Tegmental Tracts

The origin of the central tegmental tract, one of the main fiber systems of the human brain stem, from the parvocellular red nucleus and its termination in the principal olive was established by Verhaart (1936).

The medial tegmental tract was discovered by Ogawa (1939) in the cat. It arises from the region surrounding the fasciculus retroflexus, including Darkschewitsch nucleus in the rostral central gray, descends along the raphe in the ventral part of the medial longitudinal fascicle, and terminates in the MAOr and the vlPO. The presence of the two tegmental tracts, one arising from the parvocellular red nucleus, that innervates the principal olive and the other from different nuclei surrounding the fasciculus retroflexus, innervating MAOr, has been confirmed in different species, including humans (Voogd 2004).

The mesodiencephalic projections were analyzed in great detail by Onodera (1984) in the cat (Fig. 19.13). This author distinguished a series of nuclei, surrounding the fasciculus retroflexus with projections to the ipsilateral inferior olive. Darkschewitsch nucleus projects to the MAOr and less intensely to the DMCC. Bechterew's nucleus connects with the vlPO, and the parvocellular red nucleus with the dlPO. A rather vague projection of Cajal's interstitial nucleus and/or the prerubral field was found to the lateral MAOc and the VLO. A topographic arrangement was found for the parvocellular red nucleus, with its lateral portion projecting to rostral, and its medial portion to caudal dlPO. Similarly, dorsolateral Darkschewitsch nucleus projects to caudal MAOr and its ventromedial portion to rostral MAOr (Porter et al. 1993). The connections of the parafascicular region with the inferior olive in the rat were reviewed by Ruigrok (2004). Although details on this system in the rat are not known, it seems likely that its organization is very similar to that of the cat.

Strominger et al. (1979) found these connections to be very similar in monkey (Fig. 19.14), although they were not able to provide definite proof of the projection of Darkschewitsch nucleus to the MAOr; in Fig. 19.14, this projection is illustrated in analogy with the cat. The dorsomedial subnucleus of the parvocellular red nucleus, located medial to the fasciculus retroflexus, represents Bechterew's nucleus and projects to the vlPO. The main lateral and caudal parts of the parvocellular red nucleus project topographically to dlPO and llPO, with lateral

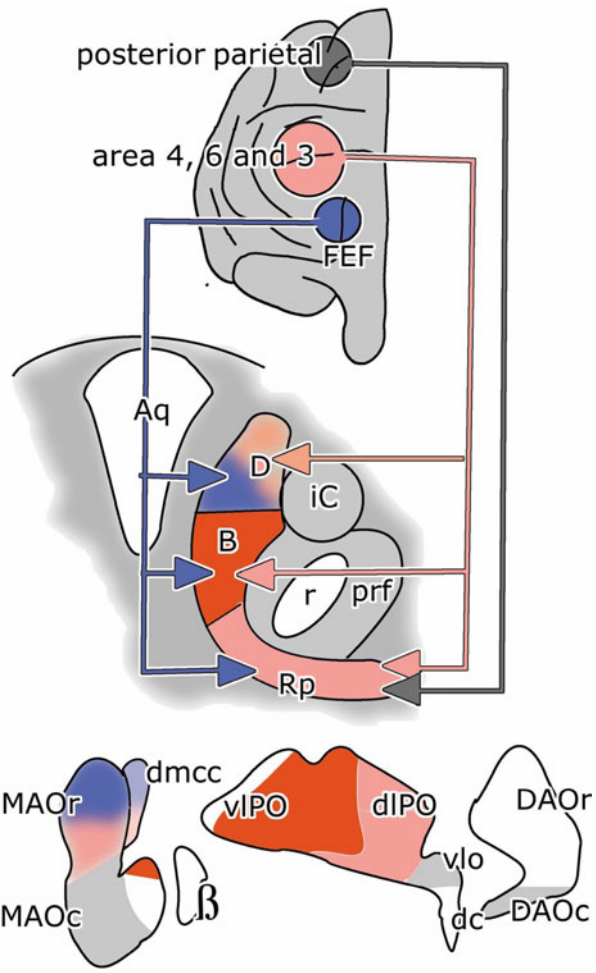

Fig. 19.13 Connections of the parvocellular red nucleus and other nuclei at the mesodiencephalic border to the inferior olive in the cat. Projections of the cerebral cortex to these nuclei are indicated in the *upper* diagram of rostral view of the cerebral hemisphere (*Lower panels* redrawn and modified from Onodera (1984)). Abbreviations: *aq* aqueduct, *B* Bechterew's nucleus, *D* Darkschewitsch nucleus, *DAOc/r* caudal/rostral dorsal accessory olive, *dc* dorsal cap, *dmcc* dorsomedial cell column, *FEF* frontal eye fields, *IC* interstitial nucleus Cajal, *MAOr/c* rostral/caudal part of medial accessory olive, *prf* prerubral field, *r* fasciculus retroflexus, *Rp* parvocellular red nucleus, *ß* group beta, *vl/dlPO* ventral/dorsal lamina of the principal olive; *Vlo* ventrolateral outgrowth

parts projecting medially in dlPO and medial parts more laterally. Thus, it transmits the somatotopical organization of this nucleus, imposed upon it by the cerebral cortex. The terminations in the PO are distributed in alternating bands of high and low density. The significance of this pattern is not known but may indicate a more precise topical organization of the system.

The preolivary nuclei at the mesodiencephalic border receive afferents from the cerebellum and from the cerebral cortex. Direct cortico-olivary connections have been observed but appear to be rather scanty (see Saint-Cyr (1983) for a review and Borra et al. (2010) for a more recent observation). Darkschewitsch' nucleus receives a cerebellar projection from the posterior interposed nucleus (Fig. 19.32a). The fastigial and dentate nuclei have been mentioned as possible afferent sources. In monkeys, the dentate nucleus projects to the parvocellular red nucleus, with

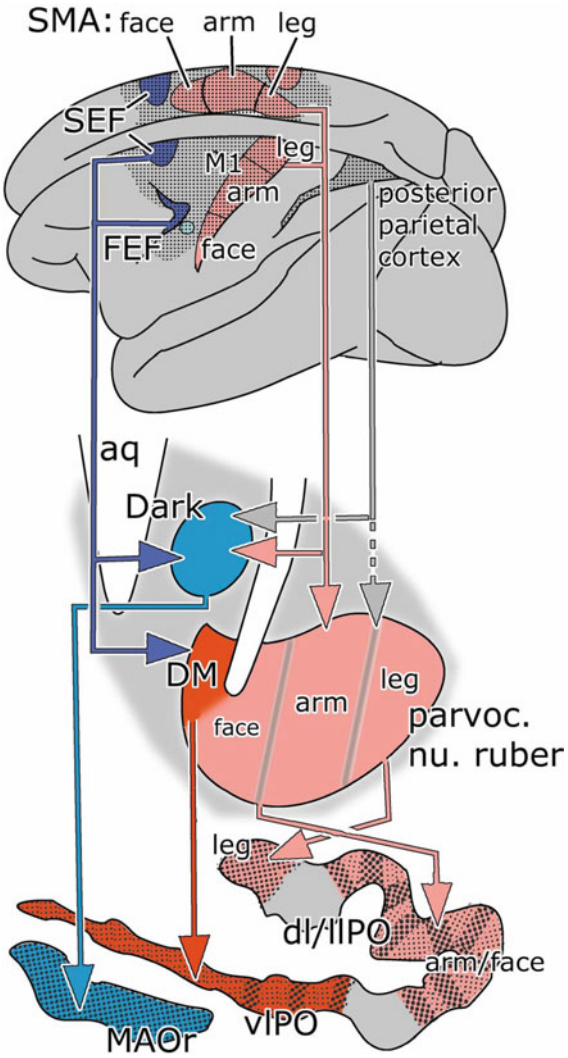

Fig. 19.14 Connections of the parvocellular red nucleus and other nuclei at the mesodiencephalic border to the inferior olive in the monkey. Origin of projections to these nuclei is indicated in the upper diagram of the cerebral hemisphere. Stippled pre- and postrolandic areas contain all neurons retrogradely labeled from the parvocellular red nucleus (Humphrey et al. 1984). Antegrade tracing was performed from frontal eye fields, primary ventral premotor, supplementary motor, and posterior parietal areas. Projections from primary motor and supplementary motor areas to the parvocellular red nucleus are somatotopically arranged. Projections to the inferior olive, illustrated in a transverse section at the bottom of the figure, were redrawn from Strominger et al. (1979). Abbreviations: *aq* aqueduct, *Dark* Darkschewitsch' nucleus, *dl/ll/vlPO* dorsal/lateral/ventral lamina of the principal olive, *DM* dorsomedial subnucleus of the parvocellular red nucleus (Bechterew's nucleus), *FEF* frontal eye field, *M1* primary motor cortex, *MAOr* rostral medial accessory olive, *SEF* supplementary eye field, *SMA* supplementary motor area

a termination from its ventrocaudal part in the dorsomedial nucleus and of its dorsal and rostral parts in its main ventrocaudal portion (Stanton 1980b; Voogd 2004) (Fig. 19.32b, c).

In the cat, cortical afferents to the nuclei of the mesodiencephalic border stem from the frontal eye fields and the areas 4, 6, and 3 (Miyashita and Tamai 1989; Nakamura et al. 1983; Saint-Cyr 1987). These areas project to Darkschewitsch' nucleus and the parvocellular red nucleus (Fig. 19.13). Afferents from posterior parietal cortex terminate in the parvocellular red nucleus (Oka 1988). Bechterew's nucleus was not considered as a separate nucleus in these studies. Through the topical projection of Darkschewitsch' nucleus to the MAOr, the rostral pole of this nucleus receives oculomotor, and its caudal part MAOr skeletomotor input (Porter et al. 1993).

The corticorubral projection has been studied in greater detail in monkeys (Fig. 19.14). The total cortical area projecting to the parvocellular red nucleus was determined by Humphrey et al. (1984) (Fig. 19.14, stippled). It includes areas 4, 6, and 8 and the posterior parietal cortex area7, extending into the dorsal bank of the intraparietal cortex. It originates from a specific set of pyramidal neurons in upper layer 4 (Catsman-Berrevoets et al. 1979). The projection of the motor cortex to the magnocellular red nucleus is differently organized: it stems from neurons in deep layer 4 and constitutes a collateral projection of the pyramidal tract. The frontal eye field projects to Darkschewitsch' nucleus and the dorsomedial subnucleus of the parvocellular red nucleus, and the supplementary eye field to the dorsomedial subnucleus only (Burman et al. 2000; Hartmann-von Monakow et al. 1979; Huerta and Kaas 1990; Huerta et al. 1986; Kuypers and Lawrence 1967; Leichnetz 1982; Leichnetz et al. 1984; Shook et al. 1990). The main lateral and caudal part of the parvocellular red nucleus receives overlapping, somatotopically arranged projections from the primary motor cortex, the supplementary motor area, and ventral and dorsal premotor area (Burman et al. 2000; Hartmann- von Monakow et al. 1979; Jürgens 1984; Kuypers and Lawrence 1967; Leichnetz et al. 1984; Orioli and Strick 1989; Tokuno et al. 1995; Wiesendanger and Wiesendanger 1985). Posterior parietal afferents mainly terminate in Darkschewitsch' nucleus; the projection to the parvocellular red nucleus is sparse (Burman et al. 2000; Faugier-Grimaud and Ventre 1989; Leichnetz 2001). Prefrontal projections from the prearcuate cortex dorsal to the principal sulcus, specifically from area 9, were noticed by Leichnetz (Leichnetz and Gonzalo-Ruiz 1996; Leichnetz et al. 1984).

Because direct connections of the cerebral cortex with the inferior olive are few, most are shunted through the nuclei of the mesodiencephalic border. Alternative pathways use other preolivary nuclei such as ventral regions of the dorsal column nuclei that may serve as a relay between the motor cortex and the DAO and the MAOc in cat and rat (Ackerley et al. 2006; Andersson 1984; McCurdy et al. 1992). This region also receives a projection from the contralateral magnocellular red nucleus. Reports on inhibition of transmission in the inferior olive by rubral or cortical stimulation (Gibson et al. 2002) may be related to the presence of GABAergic neurons in this region that project to the inferior olive (Nelson and Mugnaini 1989). Another alternative pathway for inhibition of the DAOr passes

through the anterior interposed nucleus, which receives a collateral projection from the rubrospinal tract (Huisman et al. 1983) and the nucleo-olivary pathway from this nucleus.

The Corticonuclear and Olivocerebellar Projections

The Corticonuclear Projection

The concept of the longitudinal zonal organization of the corticonuclear projection resulted from a combination of Weidenreich's subdivision of the cerebellar nuclei with observations on the presence of parasagittally oriented white matter compartments in the cerebellum of the ferret and the cat (Voogd 1964, 1969). With the Häggqvist myelin stain, bundles of medium-sized myelinated Purkinje cell axons could be distinguished in the cerebellar white matter separated by narrow slits that contain small myelinated fibers only (Fig. 19.15). Each compartment channels the Purkinje cell axons from a longitudinal Purkinje cell zone to a particular cerebellar nucleus. These Purkinje cell zones are illustrated for the ferret in Fig. 19.16. The A zone is present in the entire vermis and projects to the fastigial nucleus. The B zone occupies the lateral vermis of the anterior and posterior lobes; Deiters' lateral vestibular nucleus is its target nucleus. The C1 and C3 zones merge in the ventral anterior lobe. They extend into the simplex lobule. C3 reappears in the Crus II and terminates in the rostral paramedian lobule; C1 is present in the medial paramedian lobule. C1 and C3 project to the anterior interposed nucleus. The C2 zone extends over the entire cerebellum, from lobule II of the anterior lobe to the paraflocculus and the flocculus. It connects with the posterior interposed nucleus. The D zone occupies the lateral hemisphere. In the ansiform lobule and the paraflocculus, it is divided into the medial D1 and the lateral D2 zones that project to ventrocaudal and rotrodorsal parts of the dentate nucleus, respectively.

This longitudinal pattern in the corticonuclear projection was confirmed with retrograde axonal transport from the cerebellar nuclei (Fig. 19.17) (Bigaré 1980; Voogd and Bigaré 1980) and by Trott et al., using antegrade axonal tracing methods (Trott and Armstrong 1987; Trott et al. 1998), both in the cat. The B zone now was found to be restricted to the anterior vermis. Moreover, an injection of the lateral vestibular nucleus also produced labeled Purkinje cells in the anterior A zone (Fig. 19.17 1b). Exclusive labeling of this subpopulation was obtained from injections of the medial vestibular nucleus (Fig. 19.17 1c). In the dorsal anterior lobe, a gap between the labeled Purkinje cells in the A and B zones contains the X zone (Fig. 19.17 1c, arrow). In the anterior lobe, D1 and D2 zones are restricted to its dorsal folia. A very similar pattern in the corticonuclear projection was described for the anterior lobe of the macaque, the squirrel monkey, and the bush baby, and for the paramedian lobule and the paraflocculus of *Tupaia glis* using Nauta's silver impregnation for degenerated axons (Haines et al. 1982). White matter compartments in the macaque monkey, delineated by the accumulation of

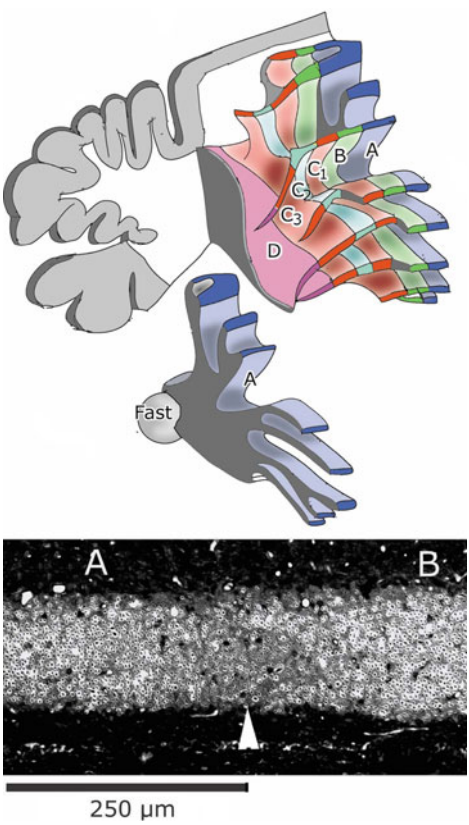

Fig. 19.15 Reconstruction of the white matter compartments in the anterior lobe of the cerebellum of the ferret. Each compartment contains the cerebellar target nucleus of the corresponding Purkinje cell zone, illustrated in the *A* compartment with the fastigial nucleus. *Bottom* photograph: border between compartments *A* and *B*. Häggqvist stain

acetylcholinesterase at the borders of the compartments, were found to be arranged like in the cat (Hess and Voogd 1986; Voogd et al. 1987a, b).

The zonal organization of the corticonuclear projection was confirmed for the rat by Buisseret-Delmas with antegrade axonal transport of horseradish peroxidase (Buisseret-Delmas and Angaut 1993). In addition to the earlier identified set of zones, they described additional X, A2, and Y zones (Fig. 19.18). The X zone is located between the A and B zones in the dorsal anterior lobe; it was first identified in electrophysiological experiments on the olivocerebellar projection (see below). It projects to cell groups located between the fastigial and posterior interposed nucleus, known as the interstitial cell groups (Trott and Armstrong 1987; Trott et al. 1998). The A2 zone is located in the medial hemisphere of the simplex lobule and the Crus II (Akaike 1992). The dorsolateral protuberance of the fastigial nucleus is the target of its corticonuclear projection. The Y zone (Buisseret-Delmas' D0 zone) projects to the dorsolateral hump of the anterior interposed nucleus. Buisseret-Delmas located the Y zone between C3 and D1. In studies of the olivocerebellar projection, it was found to occupy a more lateral position, between D1 and D2 (Fig. 19.18).

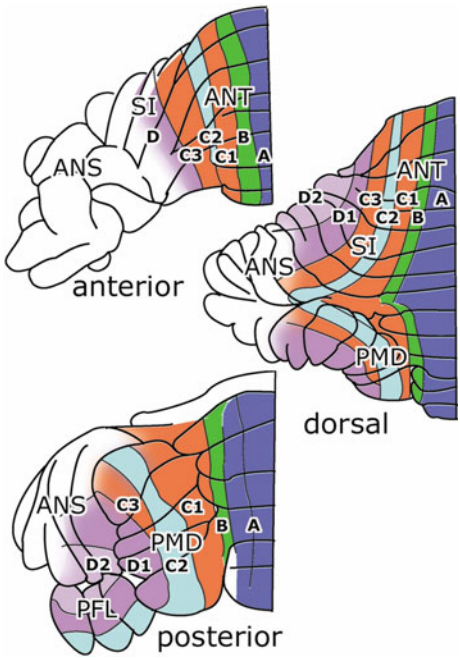

Fig. 19.16 Reconstructions of the Purkinje cell zones of the cerebellum of the ferret (Redrawn from Voogd (1969)). Abbreviations: *ANS* ansiform lobule, *ANT* anterior lobe, *PFL* paraflocculus, *PMD* paramedian lobule, *SI* simplex lobule

Another aspect of the corticonuclear projection was highlighted by the application of immunohistochemical methods, that distinguished between two populations of zonally distributed Purkinje cells, one population immunoreactive for zebrin (zebrin II: aldolase C), and a second population that was zebrin-negative. Alternating zebrin-positive and zebrin-negative bands are arranged in a reproducible pattern (Fig. 19.23). Axons of zebrin-positive Purkinje cells converge upon ventrocaudal and lateral parts of the cerebellar nuclei, and axons from zebrin-negative Purkinje cells terminate more rostrally (Fig. 19.25b). The use of the zebrin pattern as a template for the study of the olivocerebellar projection is considered in section "The Olivocerebellar Projection".

The Olivocerebellar Projection

In early morphological studies of the olivocerebellar projection, the origin of the climbing fibers from the inferior olive was not known. Axonal tracing methods visualizing the climbing fibers only became available in 1974 (Desclin 1974). Their origin from the olive had been established by Eccles et al. (1966), and Oscarsson and his group in Lund, acting on this observation, started their studies on spino-olivocerebellar climbing fiber paths (SOCPs) in the same year (Oscarsson and Uddenberg 1966).

The first attempt at a map of the topographical organization of the olivocerebellar projection was by Holmes and Steward (1908) (Fig. 19.19). It

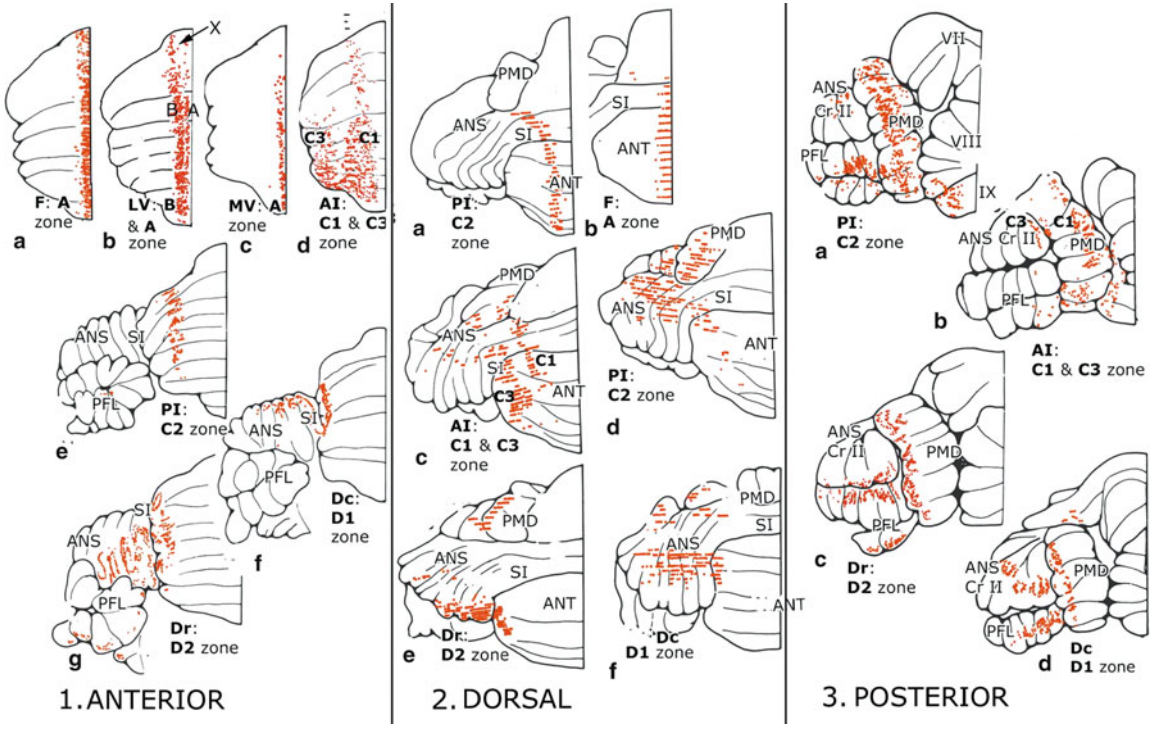

Fig. 19.17 Reconstructions of the anterior lobe (1), the dorsal aspect (2), and the posterior aspect (3) of the cerebellum of the cat, showing labeled Purkinje cells after injections of a retrograde tracer in a particular cerebellar nucleus. For each panel, the injected nucleus (**MV** medial vestibular nucleus) and the labeled Purkinje cell zone (**A** zone) is indicated (Redrawn from Bigaré (Bigaré 1980; Voogd and Bigaré 1980)). Abbreviations: *AI* anterior interposed nucleus, *ANS* ansiform lobule, *ANT* anterior lobe, *Cr I/II* Crus I/II, *Dc* caudal dentate nucleus, *Dr* rostral dentate nucleus, *F* fastigial nucleus, *LV* lateral vestibular nucleus, *MV* medial vestibular nucleus, *PFL* paraflocculus, *PI* posterior interposed nucleus, *PMD* paramedian lobule, *SI* simplex lobule

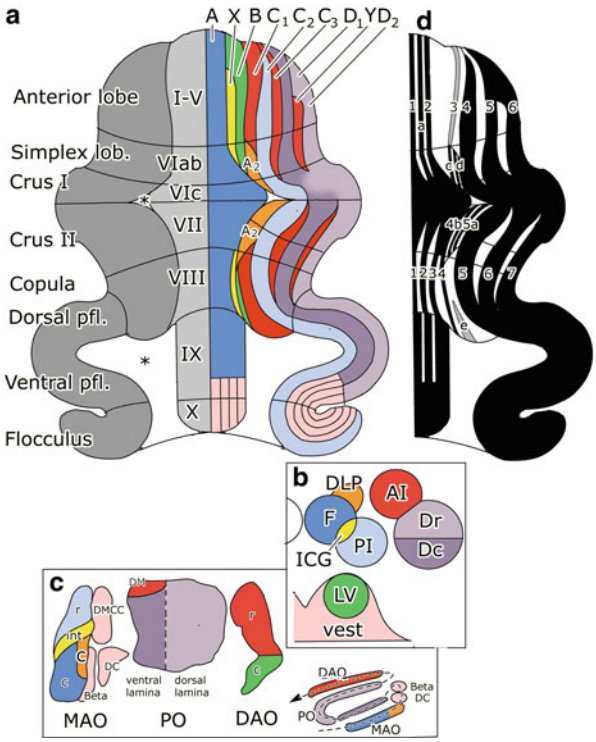

Fig. 19.18 Diagram of the zonal organization of the cerebellum of the rat. (**a**) Diagram of the flattened cerebellar cortex, the Purkinje cell zones are shown in the right half of the diagram. (**b**) Cerebellar and vestibular target nuclei of the Purkinje cell zones. (**c**) Diagram of the flattened inferior olive, showing subnuclei with projections to the Purkinje cell zones and their target nuclei. (**d**) Diagram of the zebrin-positive and zebrin-negative bands. Abbreviations: *A-D*$_2$ Purkinje cell zones A-D$_2$, *1-7* zebrin-positive bands P + 1-7, *AI* anterior interposed nucleus, *Beta* cell group beta, *c* caudal (MAO or DAO), *C* subnucleus C of the caudal MAO, *DAO* dorsal accessory olive, *Dc* caudal subnucleus of the dentate nucleus, *DC* dorsal cap and ventrolateral outgrowth, *DLP* dorsolateral protuberance of the fastigial nucleus, *DMCC* dorsomedial cell column, *DM* dorsomedial group, *Dr* rostral subnucleus of the dentate nucleus, *F* fastigial nucleus, *i* intermediate MAO, *ICG* interstitial cell groups, *LV* lateral vestibular nucleus, *MAO* medial accessory olive, *PI* posterior interposed nucleus, *PO* principal olive, *r* rostral (MAO or DAO), *vest* vestibular nuclei

remains the only diagram of its sort for the human cerebellum. The diagram shares its lobular organization with the diagrams produced for the olivocerebellar projection in rabbit and cat by Brodal 30 years later (Brodal 1940) (Fig. 19.20). Different subdivisions of the olive project to different lobules. The anterior lobe is an exception. In the rabbit, the extreme lateral portion of the anterior lobe, the "hemisphere proper," receives afferents from the rostral pole of the principal olive. The accessory olives project to the vermis and to a paravermal, intermediate zone. This tripartition was confirmed in later studies of Jansen and Brodal (1940, 1942) of the corticonuclear projection, where the vermis was found to project to the

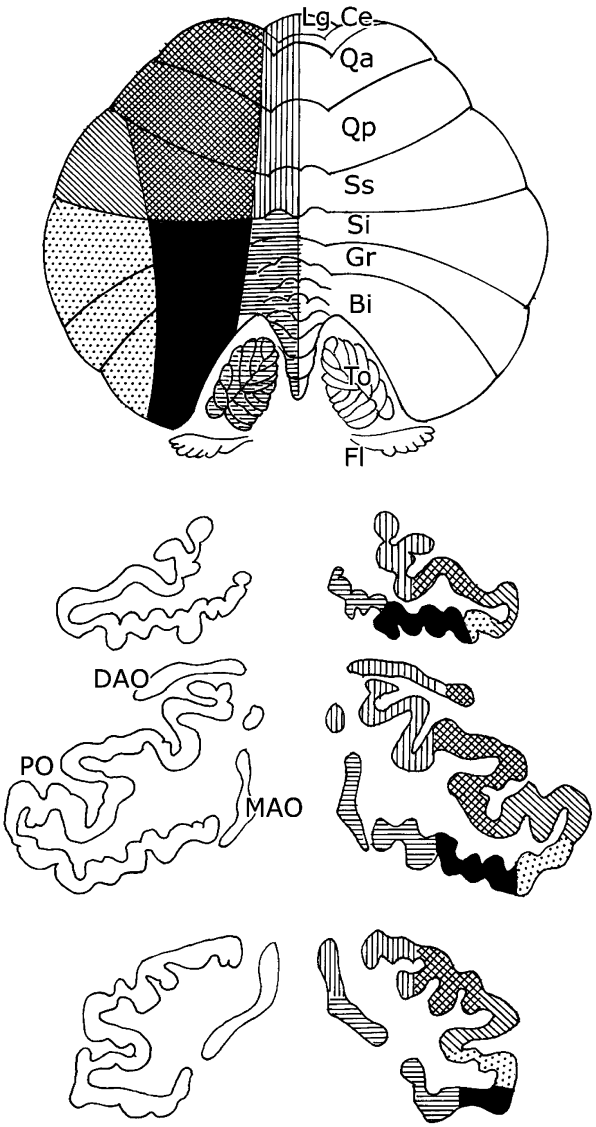

Fig. 19.19 Diagram illustrating the topographical relations between the inferior olive and the human cerebellum. The dorsal accessory olive and the medial half of the dorsal leaf of the principal olive are connected with the cortex of the superior surface of the cerebellum. Olivocerebellar fibers from the ventral lamina of the principal olive and the ventral part of the medial accessory olive project to the tonsilla and the caudal vermis (From Holmes and Steward (1908)). Abbreviations: *Bi* biventral lobule, *Ce* central lobule, *DAO* dorsal accessory olive, *Fl* flocculus, *Gr* lobulus gracilis, *Lg* lingula, *MAO* medial accessory olive, *PO* principal olive, *Qa* anterior quadrangular lobule, *Qp* posterior quadrangular lobule, *Si* inferior semilunar lobule, *Ss* superior semilunar lobule, *To* tonsilla

fastigial and the vestibular nuclei, the intermediate zone to the interposed nucleus, and the hemisphere to the lateral cerebellar nucleus. These observations lead these authors to the conclusion that olivocerebellar and corticonuclear projections are arranged according to the same zonal pattern. The three-zonal arrangement only applies to the anterior lobe and the simplex lobule. Attempts have been made to extrapolate it to the posterior lobe, but these attempts have not met with much success.

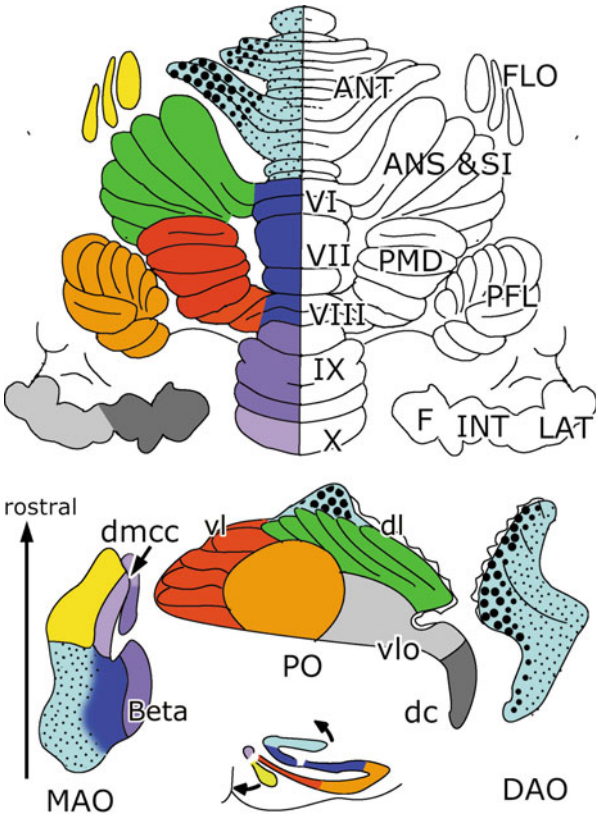

Fig. 19.20 The olivocerebellar projection in the rabbit indicated in flattened maps of the cerebellum and the inferior olive. The construction of the map of the olive is indicated in the *bottom* figurine. Olivary subnuclei and their projections are indicated with the same color (Redrawn from Brodal (1940)). Abbreviations: *ANS* ansiform lobule, *ANT* anterior lobe, *DAO* dorsal accessory olive, *dc* dorsal cap, *dl* dorsal lamina principal olive, *dmcc* dorsomedial cell column, *F* fastigial nucleus, *FLO* flocculus, *INT* interposed nucleus, *LAT* lateral cerebellar nucleus, *MAO* medial accessory olive, *PFL* paraflocculus, *PMD* paramedian lobule, *PO* principal olive, *SI* simplex lobule, *vl* ventral lamina principal olive

The conclusions of Voogd (1969) and Groenewegen and Voogd (1977) and Groenewegen et al. (1979) on the longitudinal zonal organization of the olivocerebellar projection were based on the observation that olivocerebellar fibers from subnuclei of the inferior olive use the white matter compartments to terminate on Purkinje cells of the corresponding longitudinal zone and, as collaterals, on its target nucleus. The organization of the olivocerebellar system is not a lobular but a zonal one.

Groenewegen and Voogd (1977) and Groenewegen et al. (1979) used autoradiography of [3H]leucine to map the olivocerebellar projection in the cat. Earlier, Courville and colleagues (Courville 1975; Courville and Faraco-Cantin 1978; Courville et al. 1974) had demonstrated the termination of olivocerebellar fibers in longitudinal climbing fiber zones with the same method. However, they concluded that these zones corresponded to Brodal's lobular pattern of termination. Groenewegen (Groenew(egen and Voogd 1977, Groenewegen et al. (1979) distinguished the same zones recognized earlier from their white matter compartments (Fig. 19.21). The A zone is innervated by the MAOc. It extends over the entire vermis, with the exception of lobule X that receives it climbing fibers, together with the flocculus, from the dorsal cap and the VLO. The DAOc projects to the B zone

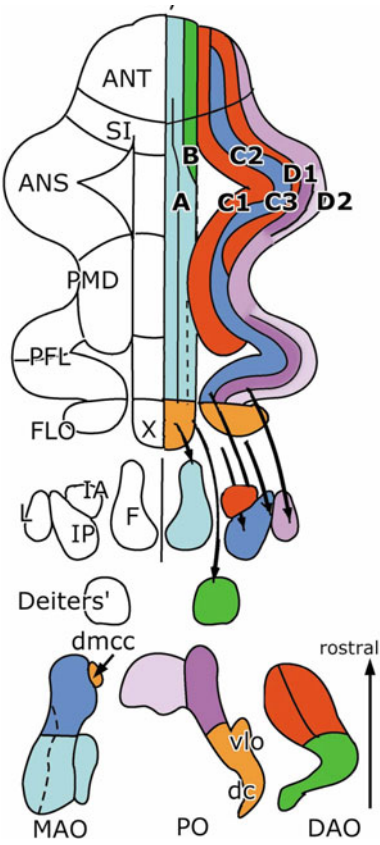

Fig. 19.21 Diagram of the zonal organization of the olivocerebellar and corticonuclear projections in the cat shown as flattened maps of the cerebellar cortex, the cerebellar nuclei and the inferior olive (Redrawn from Groenewegen et al. (1979)). Abbreviations: *ANS* ansiform lobule, *ANT* anterior lobe, *DAO* dorsal accessory olive, *dc* dorsal cap, *Deiters'* Deiters' lateral vestibular nucleus, *dmcc* dorsomedial cell column, *FLO* flocculus, *MAO* medial accessory olive, *PFL* paraflocculus, *PMD* paramedian lobule, *PO* principal olive, *SI* simplex lobule, *vlo* ventrolateral outgrowth

that is limited to the lateral vermis of the anterior lobe and the simplex lobule. C1 and C3 zones are innervated by the DAOr. They are present in the anterior lobe with the simple lobule and in the Crus II of the ansiform lobule and the paramedian lobule. C3 is restricted to the rostral paramedian lobule. Both zones fuse in the rostral anterior lobe, around the rostral extremity of the C2 zone. This zone receives its climbing fibers from the MAOr and extends over the entire cerebellar cortex, including the paraflocculus. The lateral D zone, innervated by the principal olive, also extends over the entire rostrocaudal length of the cerebellar cortex. At the level of the ansiform lobule and the paraflocculus, it is divided into D1 and D2 zones, but a differential origin of these climbing fiber subzones from the principal olive could not be established. Climbing fibers always emit collaterals to the cerebellar or vestibular target nucleus of the Purkinje cell zone they innervate. Such a collateral projection could not be identified for the projections of the VLO and the DC.

Oscarsson and his group defined their spino-olivocerebellar climbing fiber paths (SOCPs) by the spinal funiculus they use as their first link. They mapped the terminations of these paths by recording the positive climbing fiber potentials

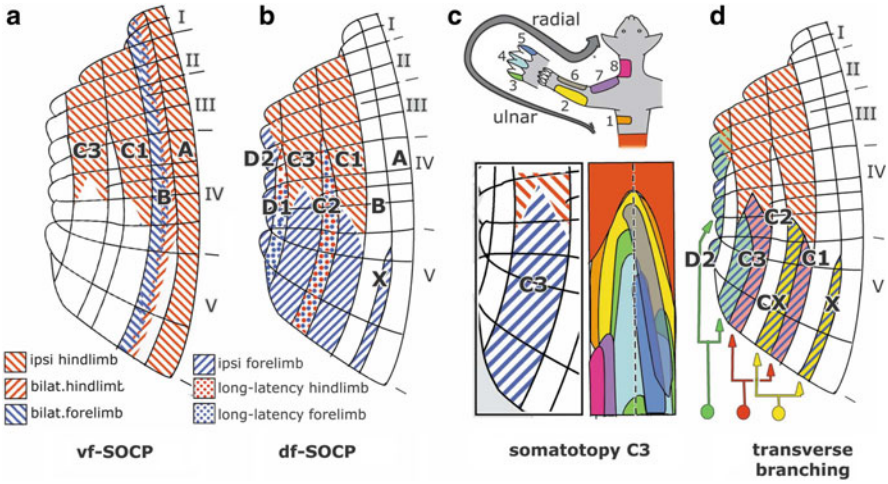

Fig. 19.22 Distribution and properties of spino-olivary climbing fiber paths (SOCPs) in the anterior lobe of the cat. (**a**) Ventral funiculus (vf)-SOCP (Redrawn from Oscarsson and Sjölund (1977b)). (**b**) Dorsal funiculus (df)-SOCP (Redrawn from Ekerot and Larson (1979a)). (**c**) Somatotopical organization of the forelimb segment of the C3 zone. Color-coded map illustrates partially overlapping, half-moon-shaped terminal fields, activated from subsequently more cranial cutaneous nerves *1–8*, indicated in *upper* figurine. *Broken line* indicates border of mirrored representations in medial and lateral C3 zone (Redrawn from Ekerot and Larson (1979b)). (**d**) Transverse branching of climbing fibers innervating dual zones (Redrawn from Ekerot and Larson (1982))

from the cerebellar surface and complex spikes from the underlying Purkinje cells from the anterior lobe and determined their laterality, somatotopical organization and the quality of their peripheral input. The ventral funiculus (vf)-SOCP takes its origin from the contralateral spinal gray, as illustrated in Fig. 19.4. It terminates in the vermis in the A zone, in the B zone, and in the C1 and C3 zones of the rostral anterior lobe (lobules I-IV). Input to the A, C1, and C3 zones stems from the hindlimb and is ipsilateral; the B zone receives a bilateral input from all limbs, with the projection of the forelimb located more laterally, partially overlapping with the projection from the hindlimb (Oscarsson and Sjölund 1977a, b; Oscarsson and Uddenberg 1966) (Fig. 19.22a). The A and B zones receive their input through the cell groups in the ventral horn and/or the intermediate gray and the MAOc and the DAOc, respectively. The hindlimb input to the C1 and C3 zones is relayed through the cell groups in the dorsal horn that are absent in the cervical enlargement. Because the ventral funiculus was isolated at the C3 segment, they missed the C1 projection to the DAOr (Fig. 19.4) and its contribution to the rostral C1 and C3 zones. Projections to the posterior lobe were rarely studied by the physiologists. The C1 zone in the paramedian lobule was found to share climbing fiber collateral input with the C1 and C3 zones in the anterior lobe (Armstrong et al. 1973; Oscarsson and Sjölund 1977a). The presence of a C3 zone in the rostral paramedian lobule was never confirmed.

The bilateral projection of the four limbs to the B zone was studied in more detail by Andersson and Oscarsson (1978). They described narrow, mediolaterally arranged longitudinal strips of Purkinje cells that receive the same climbing fiber input (i.e., mainly ipsilateral hindlimb, bilateral hindlimb, bilateral hind- and forelimb, etc., with a trigeminal microzone located most medially (Andersson and Eriksson 1981)). These "microzones" are narrow, with a width of a few Purkinje cells, but may extend for tens of millimeters in the rostrocaudal direction. The relationship of the microzones to the morphology of the climbing fiber system is discussed in ▶ Chap. 20 "Axonal Trajectories of Single Climbing and Mossy Fiber Neurons in the Cerebellar Cortex and Nucleus" (Shinoda and Sugihara).

The dorsal funiculus (df)-SOCP was studied by Oscarsson (1969) and Ekerot and Larson (1979a, b). Its first link consists of spinal root fibers ascending in the dorsal columns. Its relay in the dorsal column nuclei and its projections to the inferior olive were discussed in section "Projections from the Dorsal Column Nuclei" and illustrated in Figs. 19.7, 19.8, and 19.9. The projection to the anterior lobe is ipsilateral for all the zones. Oscarsson (1969) documented ipsilateral hind- and forelimb projections to the B zone and an ipsilateral hindlimb projection to A. These projections presumably overlap with similar projections from the vfSOCP. The relay for the B zone in the DAOc only has been substantiated for the hindlimb (Fig. 19.6). A substantial hindlimb projection from the gracile nucleus to MAOc would provide for the activation of the A zone. Ekerot and Larson (1979a, b) limited their study to the four short-latency zones, X, C1, C3, and D2, relayed monosynaptically by the dorsal column nuclei to the inferior olive, and two long-latency zones, C2 and D1, with an extra synapse, presumably in the mesencephalon (Fig. 19.22b).

The C1, C3, and D2 (or Y) zones are innervated by the DAOr. Rostral hindlimb segments of the C1 and C3 zones overlap with the vf-SOCP, and their forelimb segments extend into lobule V. A projection of this subnucleus to the D2 zone was not noticed in earlier morphological studies. Originally, the D2 zone was defined by its lateral location, its projection to the rostral dentate, and its climbing fiber afferents from the dorsal lamina of the principal olive. Although Ekerot's D2 zone is located in the most lateral part of the anterior lobe of the cat, its connections clearly differ from the original D2 zone. It should be considered as a third zone of the C1-C3 collective, innervated by the rostral DAO and projecting to the anterior interposed nucleus. The true D2 zone may have been inaccessible for the microelectrode, as it is hidden in the lateral pole of the anterior lobe of the cat, Garwicz (1997), in the ferret, proposed the neutral term Y zone for Ekerot's D2 zone. In the rat, a D0 zone (Buisseret-Delmas 1989) was identified in the lateral anterior lobe and the paramedian lobule, located between the D1 and D2 zones (Voogd et al. 2003; Sugihara and Shinoda 2004). The D0 zone occupies a similar position as the Y zone in the cat. Its connections, however, are with subnuclei that have not been identified in carnivores, receiving climbing fibers from the dorsomedial group of the ventral lamina of the principal olive and projecting to the dorsolateral hump. Moreover, it gives rise to the uncrossed descending limb of the brachium conjunctivum (Mehler 1969) that has not been identified in carnivores either.

The X zone is located between the A and B. It is a pure forelimb zone located in lobule V. It receives its climbing fibers from intermediate levels of the MAO (Campbell and Armstrong 1985) (illustrated in Fig. 19.18 for the rat). The forelimb projection from the cuneate nucleus to the intermediate MAO is illustrated in Fig. 19.6. A trigeminal input to this region is illustrated in Figs. 19.4 and 19.5.

Alternative routes for the transmission of peripheral input to the inferior olive involve the crossed ascending projections of somatosensory relay nuclei to the nuclei of the mesodiencephalic junction, referred to before. For the long-latency projection to D1, the pathway probably involves Bechterew's nucleus, a subsidiary of the parvocellular red nucleus, and the ventral lamina of the principal olive (Fig. 19.13). The pathway for the C2 zone includes Darkschewitsch' nucleus (Fig. 19.13) and the MAOr. The D1 zone displays an indistinct somatotopical organization; C2 lacks a somatotopical arrangement.

The somatotopical organization of the forelimb region of the C3 zone was studied in more detail. Climbing fibers transmitting information from cutaneous nerves terminate in partially overlapping half-moon-shaped fields in this zone. When stimulating thoracic, ulnar, radial, and neck nerves, the fields shift rostrally in this order (Fig. 19.22c). Apparently, the C3 zone contains two mirror-faced somatotopical maps in its medial and lateral halves. A similar, but single, somatotopical organization is present in the C1 and the Y (D2) zone.

Transverse climbing fiber branching was found between medial C3 and C1 and between lateral C3 and Y (D2) (Armstrong et al. 1973; Ekerot and Larson 1982) (Fig. 19.22d). Moreover, climbing fibers branch between the X zone and a new CX zone, located between C2 and C1. The presence of zonal pairs sharing the same topically arranged peripheral climbing fiber input, enclosing a zone innervated by climbing fibers carrying information descending from the mesodiencephalic junction, is a remarkable, but still unexplained feature of the anterior lobe. In rat and mouse transverse branching in the anterior lobe among the C1, C3, and D0 zones in lobules VI and VI between A and A2 and in the copula pyramidis in the C1 zone, was noticed with antegrade labeling of climbing fibers by Sugihara and Shinoda (2004) and Sugihara and Quy (2007).

Apart from tactile input, the df-SOCP climbing fibers of the df-SOCP were found to relay nociceptive input. This quality is relayed by the postsynaptic dorsal column pathway, and not by the spinal root fibers of the dorsal funiculus (Ekerot et al. 1991; Uddenberg 1968). Nociceptive input is found for the X, C1, CX, and C3 zones (Garwicz et al. 1992).

In the most recent chapter in the study of the olivocerebellar projection, the "zebrin pattern" was used as a template. Antibodies known as the zebrins exclusively stain a subpopulation of Purkinje cells in rodents that are arranged in parallel longitudinal bands, separated by bands of zebrin-negative Purkinje cells (Hawkes and Leclerc 1987) (Fig. 19.23). One of these antibodies, zebrin II, recognizes the enzyme aldolase C (Hawkes and Herrup 1995). Earlier, the same pattern was described by Scott (1964) for the enzyme 5-nucleotidase in the molecular layer of the cerebellum of the mouse. In the nomenclature devised by Hawkes, zebrin-positive bands are numbered from medial to lateral as P1+ to P7+, and the zebrin-negative bands

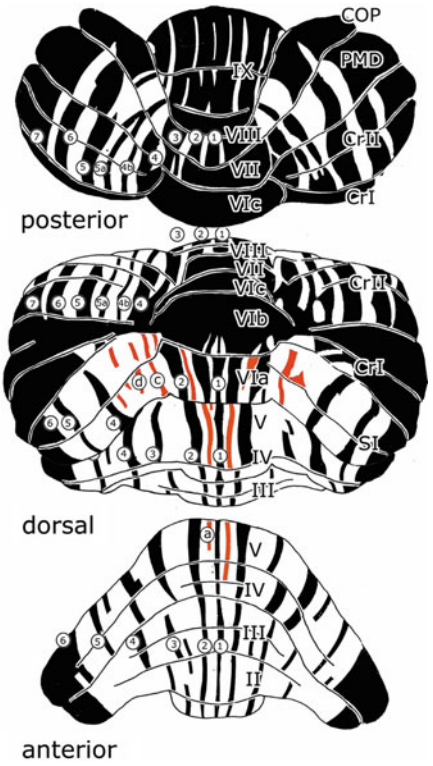

Fig. 19.23 Diagram of zebrin-positive (*black*) and zebrin-negative (*white*) Purkinje cell bands in the cerebellum of the rat. Zebrin-positive (P+) bands are numbered according to Hawkes and Leclerc (1987). Non-numbered satellite bands are shown in *red*. Abbreviations: *II-IX* lobules II-IX, *COP* copula pyramidis, *Cr I/II* Crus I/II, *PMD* paramedian lobule, *SI* simplex lobule

P1- to P6- are located lateral to the zebrin-positive bands bearing the same number (Fig. 19.23). The "satellite bands" distinguished by these authors (red in Fig. 19.23) were not numbered. Later they were found to be a reproducible feature and indicated with lower case characters (Figs. 19.18, 19.23, and 19.24).

The main question that remained was whether the zebrin-positive and zebrin-negative bands were identical to the corticonuclear and olivocerebellar projection zones. The answer to this question was provided by Voogd et al. (2003), using a bidirectional axonal tracer, injected into identified zones of the cerebellar cortex of the rat and, in much greater detail, by Sugihara c.s who mapped the olivocerebellar projection from numerous small injections of an antegrade axonal tracer in subnuclei of the inferior olive in rat (Sugihara and Shinoda 2004) and mouse (Sugihara and Quy 2007) in material counterstained for aldolase C (zebrin II). Additional studies were published by Voogd and Ruigrok (2004) and Pijpers et al. (2005). Earlier, the olivocerebellar projection in the rat had been described by Buisseret-Delmas and Angaut (1993). Their findings largely confirmed the earlier studies in carnivores. Of the additional zones described by them, the X zone receives it climbing fibers from the lateral intermediate MAOc. The A2 zone is innervated by the medial MAOc, and the Y (Delmas's D0 zone) by the dorsomedial group of the ventral lamina of the principal olive (Fig. 19.18a, c).

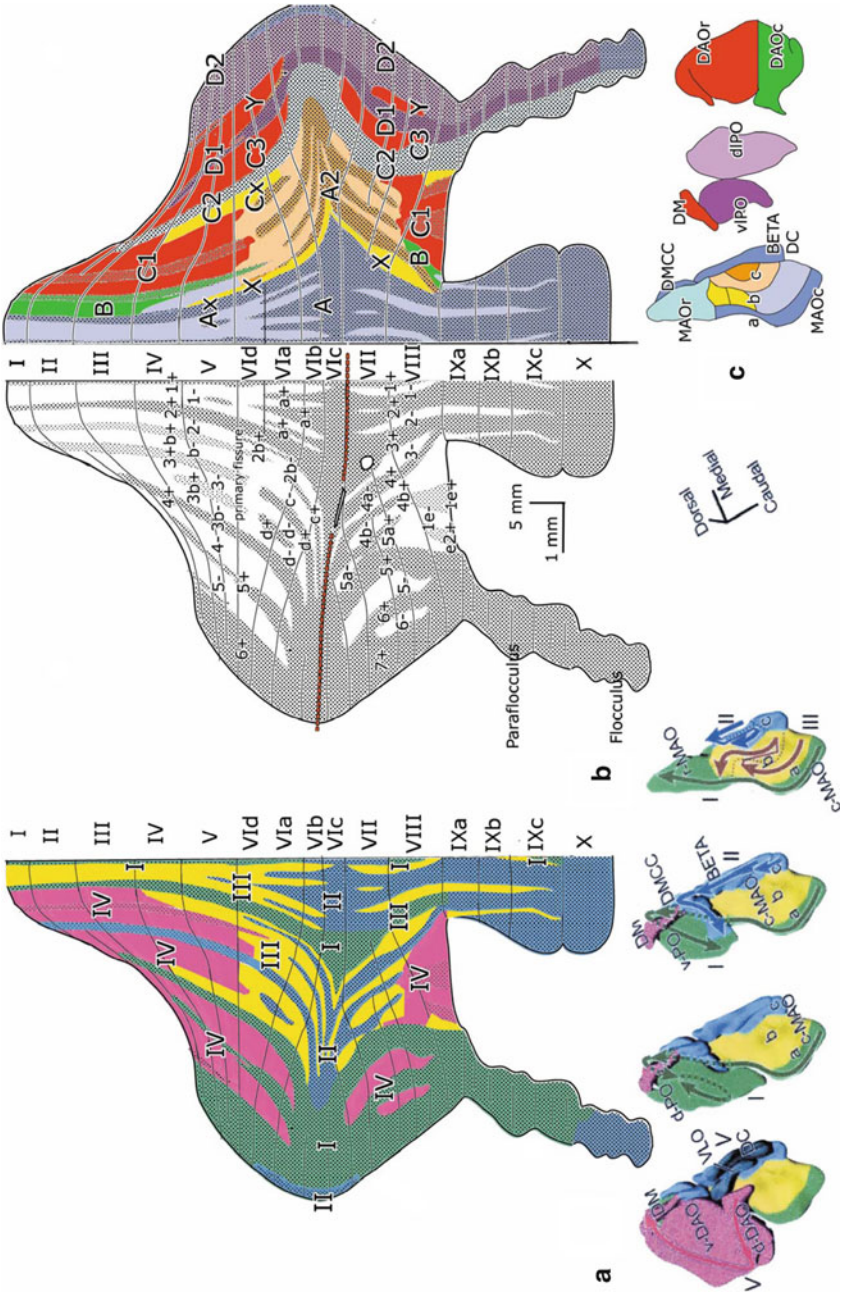

Fig. 19.24 (continued)

In Voogd's studies, the corticonuclear and olivocerebellar projection zones were found to be congruent with zebrin-positive and zebrin-negative bands. The C2, D1, and D2 zones consist of zebrin-positive Purkinje cells, and the X, B, C1, C3, and Y zones are zebrin-negative (Fig. 19.18.). Because these zebrin-negative zones are absent from the Crus I of the ansiform lobule and the paraflocculus, these lobules are entirely zebrin-positive, and the borders of the constituent C2, D1, and D2 zones cannot be distinguished. This is also the case for the X, B, and C1 zones that occupy the anterior zebrin-negative P2-band. It follows from the analysis of the olivocerebellar projection that Hawkes nomenclature for the zebrin bands in the anterior and posterior cerebellum is not consistent. Anterior bands P2+ to P6+ are continuous with posterior bands P3+ to P7+. The A2 zone occupies a region in the Crus II, containing the zebrin-positive and zebrin-negative P4b and P5a bands. Anteriorly, it corresponds to the c and d bands of the simplex lobule. In the following account, anterior and posterior bands that receive their climbing fibers from the same subdivision of the inferior olive will be indicated with their numbers separated by a dash (i.e., anterior band 2+ and posterior band 3+ are indicated as 2+/3+).

Greater detail was obtained in Sugihara and Shinoda's study (Sugihara and Shinoda 2004) of the olivocerebellar projection in the rat. They distinguished four groups in this projection (Fig. 19.24a, b). Group I (green) includes the lateral subnucleus a of the MAOc, the MAOr, and the principal olive. It projects to zebrin-positive bands P1, with the exception of lobule VII, 2+/3 + and to the 4+/5+, 5+/6+ and 6+/7+. With the exception of subnucleus a of the MAOc that receives somatosensory input, it receives its afferents from the nuclei at the mesodiencephalic junction. Group II (blue) comprises the projections of caudal subnucleus c of the MAOc, group beta and the DMCC and the caudal part of the dorsomedial group to zebrin-positive bands a+/2+, 3+, and 4+ in the uvula and a complicated array of zebrin-positive bands in intermediate regions of lobule VI-VIII (2b+, c+, d+, 4b+, 5a+). Of this group, the beta nucleus and the DMCC receive vestibular input, and lateral MAOc shares the tecto-olivary projection with the group III and receives a spatially segregated somatosensory afferents. Group III (yellow) includes the projections of subnucleus c of the MAOc to zebrin-negative bands in the vermis and in intermediate regions of lobules VI-VIII. In group IV (red), the DAO and the rostral part of the dorsomedial group project to anterior bands 2-, b+ and -, 3+ and -, 3b+ and -, 4- and 5- and posterior 4-, e1 and 2+ and -, 5- and 6-. This region includes

Fig. 19.24 (**a**) Olivocerebellar projections to aldolase-C-positive and aldolase-C-negative Purkinje cell zones. The four groups in this projection, their origin from the olive and their termination in the cortex, are indicated in different colors. Group I (*green*) and group II (*blue*) project to aldolase-positive bands. Group III (*yellow*) and group IV (*red*) project to aldolase-negative bands. (**b**) Flattened reconstruction of the cerebellar cortex showing aldolase-C-positive and aldolase-C-negative bands. (**c**) Correspondence of aldolase C banding pattern with A-D zones and their origin from the inferior olive. The **A** and **A2** zones correspond with multiple aldolase-C-positive (*dark blue* and *dark orange*) and aldolase-C-negative (*light blue* and *light orange*) bands (**a** and **b**, Redrawn from Sugihara and Shinoda (2004))

both zebrin-negative, and the weakly zebrin-positive bands 3+ and 3b+ in the anterior cerebellum and e1, and e2 in the posterior cerebellum. Group IV is purely somatosensory.

The correspondence between the four groups of Sugihara and Shinoda (2004) and the nomenclature of Voogd (Fig. 19.18) and Buisseret-Delmas (1993) is indicated in Fig. 19.24C. The localization of X, B, C1-3, Cx and the D1, Y, and D2 zones is immediately clear. The position of the D1 and D2 zones, flanking the Y (Buiseret-Delmas's D0 zone), now was definitely established. The possibility still exists that D1 is discontinuous in the Crus I (lobule VIc) because no labeling was observed in this region with injections of the vlPO. The main difference with previous maps is the composition of the A and A2 zones of an array of interdigitating zebrin-positive and zebrin-negative bands.

The principle, formulated by Groenewegen et al. (1979) that olivocerebellar fibers emit collaterals that terminate in the target nucleus of the Purkinje cells innervated by these fibers, has not been challenged.

The collateral olivocerebellar projection to the cerebellar nuclei was studied in the rat by Ruigrok and Voogd (2000) and Sugihara and Shinoda (2007). The collateral projections of subnuclei of the inferior olive were found to overlap with the corticonuclear projections from the Purkinje cell zones that receive climbing fibers from these subnuclei, as reviewed in the previous paragraphs.

Zebrin (aldolase C) immunochemistry cannot be used to map the corticonuclear projection of the individual zones. However, it may serve to visualize the overall topography of the corticonuclear projection of zebrin-(aldolase C)-positive and negative Purkinje cell zones as labeling of fibers and terminals in the cerebellar nuclear neuropil (Hawkes and Leclerc 1986; Sugihara and Shinoda 2007). Zebrin-positive and zebrin-negative zones that interdigitate in the cerebellar cortex, converge upon two separate homogeneously zebrin-positive or zebrin-negative regions of the cerebellar nuclei, that occupy caudoventral and lateral, and rostrodorsal parts of the nuclei, respectively (Fig. 19.25b). As a result, the medial (fastigial) nucleus is divided into the rostrodorsal, zebrin-negative and caudoventral, zebrin-positive parts, which may be related to some functional localization in this nucleus. In the interposed nucleus, this division between the rostrodorsal and caudoventral parts roughly corresponds to the division between the anterior and posterior interposed nuclei. The lateral (dentate) nucleus is entirely aldolase-C-positive, in accordance with its innervation by zebrin-positive bands only.

Collateral projections to the fastigial nucleus from groups I and II that innervate zebrin-positive zones include those from subnucleus a of the MAOc (green in Fig. 19.25), group beta and DMCC (light blue), and subnucleus c (dark blue). These collateral projections occupy subsequently more dorsal and rostral laminae (Fig. 19.25a, b, g, h). The collateral projection of subnucleus c to lobules VI and VII, the so-called visual vermis, demarcates the visuomotor subdivision of the fastigial nucleus. Subnucleus b of the MAO that belongs to group III, which innervates zebrin-negative territory, supplies collateral projections to the rostral and dorsal fastigial nucleus. Olivocerebellar fibers from medial subnucleus b that innervate the zebrin-negative bands of the A2 zone emit collaterals to

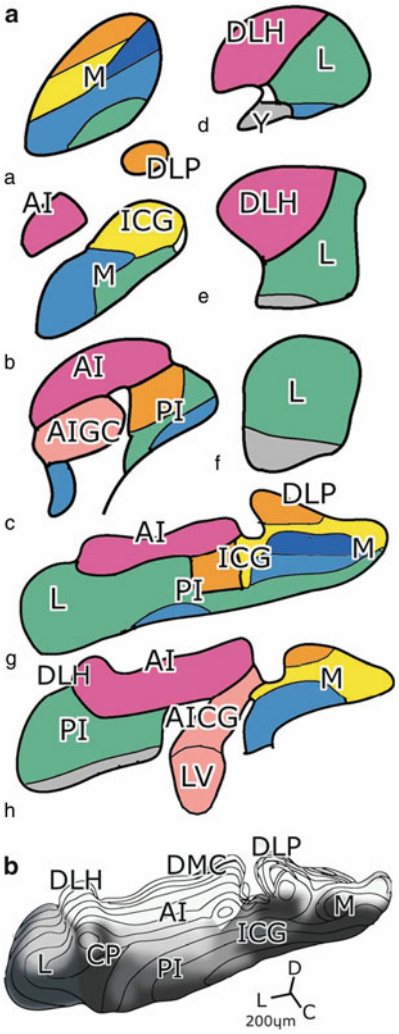

Fig. 19.25 (**a**) Collateral projections of olivocerebellar fibers to the cerebellar nuclei in the rat illustrated in diagrams of parasagittal (*a–f*) and transverse sections (*g*, *h*). Projections from the four groups in the olivocerebellar projection, distinguished in Fig. 19.24a, are shown in the same colors. Within group II, the projection to lobules VI and VII (the "visual vermis": *dark blue*) is distinguished from other lobules (*light blue*). Within group III, the projections of the dorsolateral protuberance and medial posterior interposed nucleus (orange) are distinguished from those to rostral fastigial nucleus and interstitial cell groups (*yellow*). (**b**) Caudal view of a 3-D reconstruction of the caudoventral and lateral aldolase-C (zebrin-positive) and rostral aldolase-C-negative compartments of the cerebellar nuclei of the rat (Redrawn from Sugihara and Shinoda (2007)). Abbreviations: *AI* anterior interposed nucleus, *AICG* anterior interstitial cell groups, *C* caudal, *CVP* caudal pole, *D* dorsal, *DLH* dorsolateral hump, *DLP* dorsolateral protuberance, *DMC* dorsomedial crest, *ICG* interstitial cell groups, *L* lateral cerebellar nucleus, *LV* lateral vestibular nucleus, *M* medial cerebellar nucleus, *PI* posterior interposed nucleus

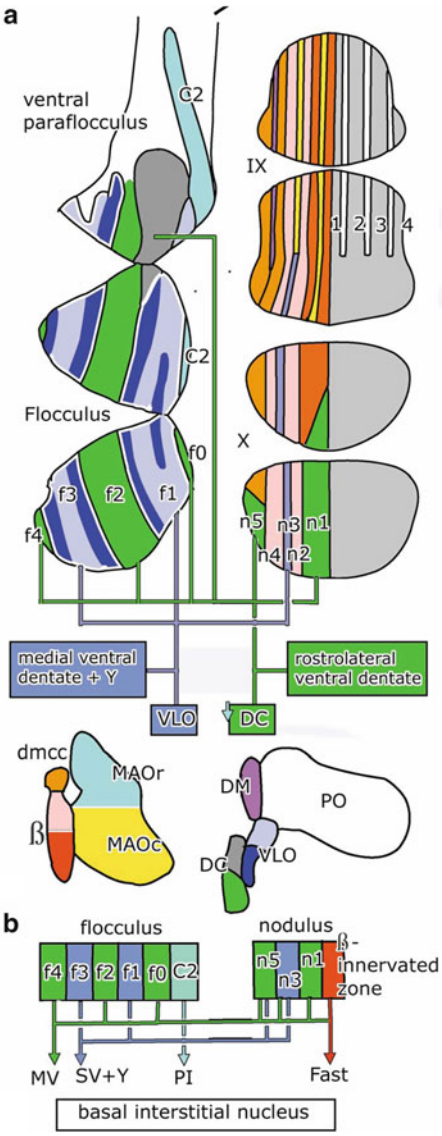

Fig. 19.26 Afferent climbing fiber and efferent projections of the flocculus and the nodulus and adjacent lobules. (**a**) Zonal organization of the olivocerebellar projection to the flocculus and the adjacent ventral paraflocculus and to the nodulus and the uvula in the rat and their origin from the inferior olive, shown in flattened diagrams of these structures. (**b**) Efferent connections of the flocculus and the nodulus in rabbits. Note different localization of group beta innervated zone in the nodulus of rat and rabbit. Abbreviations: *DC* dorsal cap, *DM* dorsomedial group, *f0-f4* floccular zones f0-f4, Fast, fastigial nucleus, *MAOc/r* caudal/rostral medial accessory olive, *MV* medial vestibular nucleus, *n1-n5* nodular zones 1–5, *PI* posterior interposed nucleus, *PO* principal olive, *ß* group beta, *SV* superior vestibular nucleus, *VLO* ventrolateral outgrowth, *Y* group Y

the dorsolateral protuberance and spill over in the adjacent posterior interposed nucleus (orange). Lateral subnucleus b innervates the base of the DLP and the interstitial cell groups (yellow). The latter represents the collateral projection of the X zone. Collateral projections from the MAOr and the ventral and dorsal laminae of the PO, that belong to group I (green), terminate in the zebrin-positive neuropil of the posterior interposed nucleus and in the caudal and rostral portions of the dentate nucleus, respectively. Collateral projections of

group IV include those of the DAOr that innervate the anterior interposed nucleus (red), and the DAOc that provide collaterals to the lateral vestibular nucleus and to islands of gray matter between the anterior interposed and lateral nuclei, known as the anterior interstitial cell groups (AICG, pink). The neuropil of the target nuclei of group IV is devoid of zebrin-positive elements.

Olivocerebellar projections to the flocculus and the nodulus and neighboring lobules have received much attention. In the flocculus of the rabbit, five Purkinje cell zones and corresponding white matter compartments could be distinguished (Tan et al. 1995a, b, c) (Fig. 19.26a). The caudal extension of the C2 zone is located along its lateral border. Actually, this lateral border corresponds to the inner, medial border of the folial chain of the hemisphere that is turned back upon itself as the flocculus. The f1 and f3 zones receive a projection from the rostral dorsal cap (DC) and the ventrolateral outgrowth (VLO), the f2 and f4 zones from the caudal DC. In the flocculus of the rat, the C2 zone and the four floccular zones, with the same dual projection from the DC and the VLO, could be distinguished (Ruigrok et al. 1992). A fifth DC-innervated f0 zone was identified by Sugihara et al. (2004) (Fig. 19.26a). A differential projection of caudal and rostral parts of the VLO was found by these authors, confirming earlier observations by Gerrits (1982) in the cat. A similar zonal organization is present in the flocculus of the mouse (Schonewille et al. 2006). In monkeys, the f4 zone appears to be absent (Voogd et al. 1987a, b). In all species, the floccular zones extend for some distance on the ventral paraflocculus. In the rabbit, this extension is known as folium P (Yamamoto 1978, 1979), in the cat as the medial extension of the ventral paraflocculus (ME: Gerrits and Voogd 1982), and in monkeys, the floccular zones occupy the entire ventral paraflocculus (Voogd et al. 1987b).

Collateral projections from the DC terminate in the rostrolateral ventral dentate nucleus, from the VLO in its medial part and in the dorsal group Y (Sugihara et al. 2004). Climbing fibers from the VLO also terminate in the extreme lateral part of the ansiform lobule (Fig. 19.24). Olivocerebellar fibers from DC and VLO do not collateralize to the vestibular nuclei (Ruigrok and Voogd 2000; Sugihara et al. 2004). Collateral projections from the group beta and a lateral part of subnucleus b of the MAOc to parts of the vestibular nuclei were identified by Ruigrok (unpublished) and Sugihara and Shinoda (2007), respectively.

The zonal organization of the nodulus and the uvula is fairly complicated. In the uvula, four zebrin-positive bands are present, separated by narrow zebrin-negative slits. These zebrin-negative slits disappear in the ventral uvula. Purkinje cells in the ventral uvula and the nodulus are all zebrin-positive (Fig. 19.26) (Voogd et al. 1996). In the medial and lateral uvula, the n1 and n5 zones are innervated by the DC, and an intermediate N3 band receives climbing fibers from the VLO. Of these zones, only n3 continues into the ventral uvula. In the uvula, the caudal group beta innervates zebrin-positive band P1+ and medial P2+, rostral group beta innervates lateral P2+ and medial

P3+, and climbing fibers terminating in lateral P3+ and in P4+ are derived from the DMCC. The narrow P1-, P2-, and P3- bands receive climbing fibers from subnucleus b of the MAOc. According to Sugihara and Shinoda (2004), climbing fibers terminating in P4+ are derived from the caudal part of the dorsomedial group and the most caudal and medial part of the vlPO and the dorsomedial group is an alternative source for the P3- projection. The localization of the DC and VLO-innervated zones was confirmed for the rat by Ruigrok (Ruigrok 2003), who also demonstrated collateralization of climbing fibers between the projections from the DC to the rostral DC-innervated zone in the ventral paraflocculus and the n1 and n5 zones in the nodulus and for the VLO between f1 and f3 and n3.

The efferent connections of the Purkinje cell zones of the flocculus and the nodulus have been studied in rabbits (Fig. 19.26b). The DC-innervated f2 and f4 zones project to oculomotor relay cells in the medial vestibular nucleus, the VLO-innervated f1 and f3 zones project to oculomotor relay cells in the group Y and the superior vestibular nucleus (De Zeeuw et al. 1994b; Tan et al. 1995a). The zonal organization of the rabbit nodulus differs from the rat in the presence of a medial beta-innervated zone, but DC and VLO-innervated N1, N3, and n4 zones are present in the same configuration as in the rat. All the zones project to the medial vestibular nucleus; additional projections to the superior vestibular nucleus and group Y take their origin from n3 and n4 (Wylie et al. 1994). Terminations in the superior and medial vestibular nuclei are complementary to those from the flocculus (Angaut and Brodal 1967; Haines 1977; Voogd 1964). All or most of the Purkinje cell zones of the flocculus and the nodulus project to the basal interstitial nucleus.

The Nucleo-olivary Pathway

The pathway from the cerebellar nuclei to the contralateral inferior olive was discovered by Graybiel et al. (1973) in the cat. It takes its origin from the small, GABAergic neurons in all cerebellar nuclei (Mugnaini and Oertel 1985). The projection is reciprocal with respect to the collateral projections of the subnuclei of the inferior olive to the cerebellar nuclei and has been described in the rat (Ruigrok and Voogd 1990), the cat (Courville et al. 1983a; Legendre and Courville 1986; Tolbert et al. 1976), and the monkey (Beitz 1976; Chan-Palay 1977b; Kalil 1979). Nucleo-olivary fibers from the dentate and interposed nuclei ascend in a separate bundle, ventral to the brachium conjunctivum, decussate caudal to the brachium, and descend in the tegmentum to the olive. Nucleo-olivary fibers from the fastigial nucleus take a more diffuse route to the olive (Legendre and Courville 1986). GABAergic projections from the vestibular nuclei and the group Y to the DC, VLO, the group beta, and the DMCC were considered in section "Optokinetic and Vestibular Projections to the Inferior Olive". In the rat, small numbers of fibers recross at the level of the olive. Recrossing fibers mainly terminate in MAOr, vlPO,

Fig. 19.27 White matter compartments in the anterior lobe of *Macaca fascicularis*. Processed for acetylcholine esterase. Abbreviations: *IntA* anterior interposed nucleus; *bc* brachium conjunctivum, *cr* restiform body

and in the dorsomedial group (Ruigrok and Voogd 1990). In all species, a projection from the ventrocaudal dentate to the vlPO, and from the rostral dentate to the dlPO, was found.

Olivocerebellar and Corticonuclear Projections in Primates

The presence of corticonuclear projection zones A-D in prosimians, macaques, and squirrel monkeys was demonstrated by Haines and his colleagues for the anterior lobe of these species (Haines et al. 1982). A division of the D zone into D1 and D2 zones was not observed by these authors. The parasagittal organization of white matter compartments in the macaque cerebellum, visualized by the accumulation of acetylcholinesterase at their borders, was found to be very similar to earlier observations in carnivores (Voogd et al. 1987a) (Fig. 19.27). An X compartment was recognized in the anterior cerebellum; D1 and D2 compartments that issue at the caudal and more rostral portions of the dentate nucleus were recognized in the dorsal paraflocculus and the paramedian lobule. In experiments using autoradiography of antegradely transported tritiated leucine, the A, X, B, and C2 compartments were shown to channel the olivocerebellar fibers to their respective Purkinje cell zones.

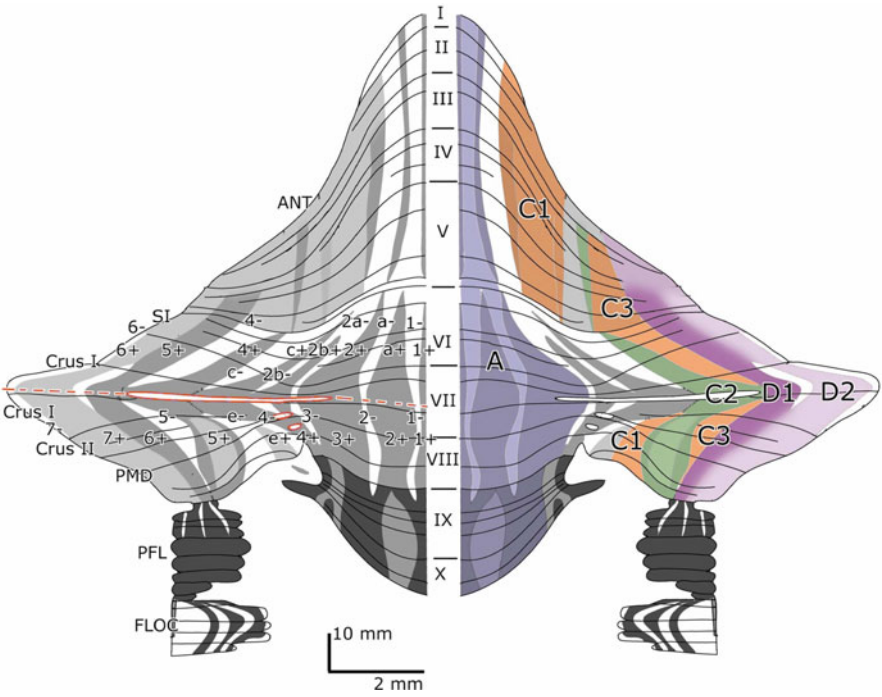

Fig. 19.28 Aldolase-C-positive and aldolase-C-negative bands in a flattened reconstruction of the cerebellar cortex of the marmoset (*left*). The correspondence with the *A*, *C1*, *C2*, *C3*, *D1*, and *D2* zones, based on the afferent climbing fiber and efferent nuclear connections of the aldolase-C-positive and aldolase-C-negative bands, is indicated in the *right hand panel*. The symmetry axis for the numbering of the bands and the areas without cortex in the center of the ansiform loop are shown in *red* (Redrawn from Fujita et al. (2010)). Abbreviations: *ANT* anterior lobe, *FLO* flocculus, *PFL* paraflocculus, *PMD* paramedian lobule, *SI* simplex lobule, *I-X* lobules I-X

Knowledge of the corticonuclear and olivocerebellar projections in subhuman primates remains fragmentary, particularly with respect to the connections of the dentate nucleus. A major advance was the publication of a complete map of the aldolase-C (zebrin II)-positive and negative bands in the marmoset, a small primate (Fujita et al. 2010) (Fig. 19.28). For the vermis, the zebrin pattern in primates was analyzed by Sillitoe and colleagues (2005), but the hemisphere remained unexplored. The banding pattern of the marmoset cerebellum is very similar to the rat (Fig. 19.24). A, C1, C2, C3, D1, and D2 zones could be recognized using small injections of bidirectional tracers in specific aldolase-C-positive or aldolase-C-negative bands. D1 receives a projection from the vlPO and D2 from the dlPO. In the posterior lobe, the P5a bands appear to be absent. In the rat, these bands are part of the A2 zone. The target of the P5a- band, the dorsolateral protuberance of the fastigial nucleus, is not present in the marmoset either. A reduction of the A2 zone in this species, therefore, appears likely.

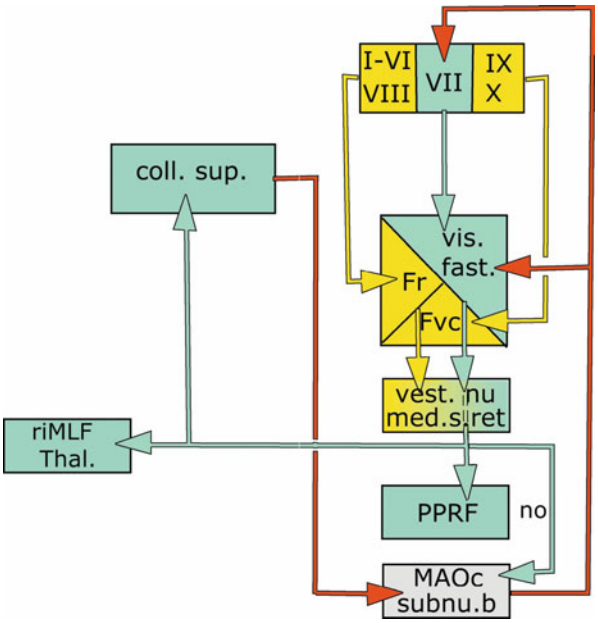

Fig. 19.29 Diagram of the projections of the fastigial nucleus. Projections of the rostral and ventrocaudal fastigial nucleus are indicated in *yellow* and those from its visuomotor division in *green*. The recurrent climbing fiber pathway from the superior colliculus is shown in *red*. Abbreviations: *coll.sup* superior colliculus, *Fr* rostral division fastigial nucleus, *Fvc* ventrocaudal division fastigial nucleus, *I-X* vermal lobules I-X, *MAOc* caudal medial accessory olive, *med.s.ret* medial reticular formation, *no* nucleo-olivary pathway, *PPRF* pontine paramedian reticular formation, *riMLF* rostral interstitial nucleus of the medial longitudinal fascicle, *vest.nu* vestibular nuclei, *vis.fast* visuomotor division fastigial nucleus

The Cerebellar Nuclei: Efferent Connections and Recurrent Climbing Fiber Paths

The Fastigial Nucleus

The fastigial nucleus receives projections from the anterior vermis and lobule VIII in its rostral portion, from the oculomotor vermis (lobule VII) in a caudal subdivision, and from lobules IX and X in its ventrocaudal part (Fig. 19.29). In rodents, a dorsolateral protuberance is present that receives Purkinje cell axons from the A2 zone (Buisseret-Delmas 1988) (Fig. 19.18). The rostral fastigial nucleus projects bilaterally and symmetrically to the vestibular nuclei (magnocellular medial and descending vestibular nuclei, nucleus parasolitarius) and the medial bulbar and pontine reticular formation (Batton et al. 1977; Homma et al. 1995; Teune et al. 2000). The entire contralateral projection uses the uncinate tract (Thomas 1897) that decussates in the cerebellar commissure and hooks over the brachium conjunctivum to enter the vestibular nuclear complex from laterally. It emits an

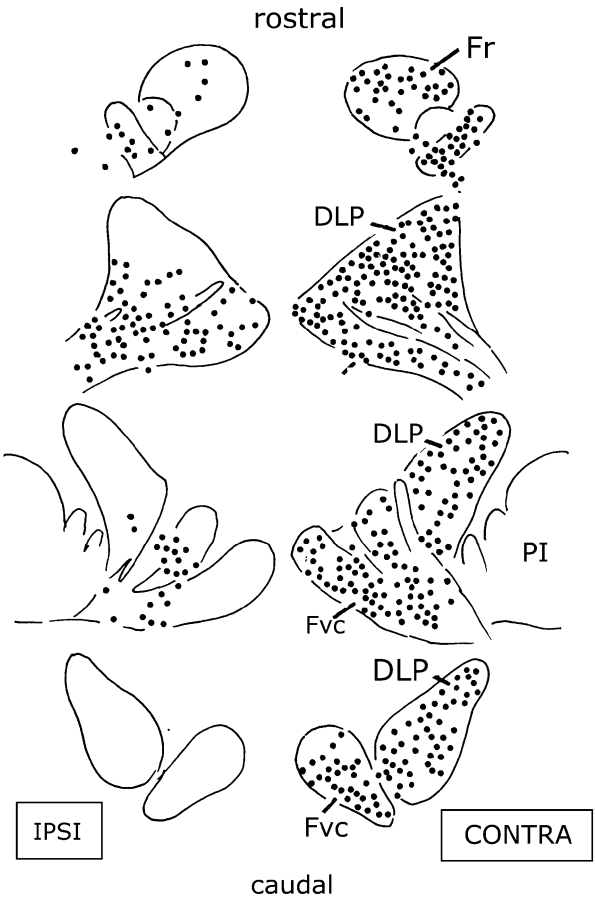

Fig. 19.30 Labeled neurons in the rat fastigial nucleus from an injection of a retrograde tracer affecting the entire left-sided output of the nucleus. Abbreviations: *DLP* dorsolateral protuberance, *Fr* rostral fastigial nucleus, *Fvc* ventrocaudal fastigial nucleus, *PI* posterior interposed nucleus

ascending branch (Probst 1901) consisting of scattered fibers around the medial pole of the brachium, that does not join it in its decussation. The direct fastigiobulbar tract enters the vestibular nuclei from medially. In the mouse, the ipsilateral pathway was found to originate from glycinergic neurons (Bagnall et al. 2009). The distribution of these glycinergic cells in the ventral and rostral fastigial nucleus in the mouse corresponds closely to the neurons with ipsilateral projections in the rat (Fig. 19.30). The projections of the caudal fastigial nucleus and the dorsolateral protuberance are entirely crossed.

The connections of the caudal, oculomotor division of the fastigial nucleus have been studied mainly in monkeys (Noda et al. 1990) (Fig. 19.29). This subdivision appears to be the main source of the crossed ascending branch of the uncinate tract. Its bilateral projection to the vestibular nuclei and the bulbar reticular formation overlaps with the rostral fastigial nucleus. Specific contralateral projections of the oculomotor division include the pontine paramedian reticular formation (PPRF)

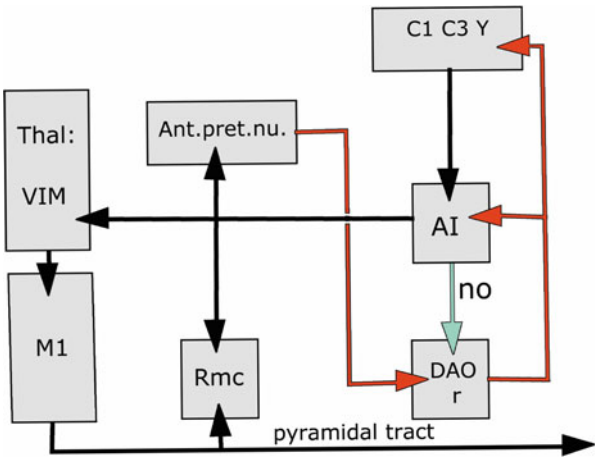

Fig. 19.31 Diagram of the projections of the anterior interposed nucleus. The recurrent climbing fiber pathway from the pretectum is indicated in *red*. Abbreviations: *AI* anterior interposed nucleus, *Ant.pret.nu* anterior pretectal nucleus, *DAOr* rostral dorsal accessory olive, *M* primary motor area, *no* nucleo-olivary pathway, *Rmc* magnocellular red nucleus, *Thal* thalamus, *VIM* ventral intermediate thalamic nucleus

that contains the excitatory and inhibitory burst cells for horizontal eye movements, the rostral interstitial nucleus of the medial longitudinal fascicle (riMLF) with similar neurons for vertical eye movements, the rostral intermediate layer of the superior colliculus, where fibers cross in the tectal commissure to innervate the contralateral side (May et al. 1990), and parts of the suprageniculate, ventral intermediate, ventral lateral and intralaminar thalamic nuclei.

A recurrent tecto-olivary pathway takes its origin from the intermediate layer of the superior colliculus to terminate in the contralateral medial MAOc (Figs. 19.12 and 19.30). In all species, this subnucleus projects to the oculomotor vermis. In rodents, the tecto-olivary pathway also innervates a separate neuronal population in subnucleus b of the MAOc that projects to the A2 zone and its target nucleus, the dorsolateral protuberance (Akaike 1992; Ruigrok and Voogd 2000). The contralateral projection of the dorsolateral protuberance to the brain stem is mainly directed at the lateral, parvocellular reticular formation and the adjoining spinal nucleus of the trigeminal nerve, the parabrachial nuclei, the nucleus pedunculopontinus, and the deep mesencephalic nucleus. This system appears to absent or rudimentary in primates and carnivores.

Anterior Interposed Nucleus

Projections from the anterior and posterior C1, C3, and Y zones converge on to the anterior interposed nucleus, where they are arranged into a single somatotopical map (Garwicz and Ekerot 1994). The main projections of the anterior interposed nucleus include the magnocellular red nucleus, the nucleus reticularis tegmenti pontis, and, through the ventral intermediate and ventral lateral thalamic nuclei, the primary motor cortex (Fig. 19.31). A recurrent pretecto-olivary pathway arises from the anterior pretectal nucleus and relays in the DAOr (Kawamura and Onodera

1984; Kawamura et al. 1982; Sugimoto et al. 1982) (see also section "Afferents from Tectum and Pretectum" and Figs. 19.12 and 19.31).

In rodents, the dorsolateral hump (Goodman et al. 1963) (Fig. 19.1) may be considered as a subnucleus of the anterior interposed nucleus. It receives a projection of the D0 zone, the presumed equivalent of the Y zone in the cat (Sugihara et al. 2009) (Fig. 19.18). The D0 zone and the dorsolateral hump are innervated by the dorsomedial group of the ventral lamina of the principal olive. The dorsolateral hump gives origin to the uncrossed descending branch of the superior cerebellar peduncle (Cajal 1972; Mehler 1969). It terminates in the lateral parvocellular reticular formation and the adjoining spinal nucleus of the trigeminal nerve (Teune et al. 2000), where it overlaps with terminals of the contralateral dorsolateral protuberance. Both of these systems appear to be absent in non-rodent species.

Posterior Interposed Nucleus and Interstitial Cell Groups

The posterior interposed nucleus is the recipient of Purkinje cell axons of the C2 zone that extends over the entire rostrocaudal length of the cerebellar cortex from lobule III into the flocculus. The MAOr provides the C2 zone with its climbing fibers and the posterior interposed nucleus with a collateral projection. The MAOr receives its descending input through the medial tegmental tract from Darkschewitsch nucleus located at the mesodiencephalic junction (Ogawa 1939). This nucleus is a relay in the projection from frontal eye fields to the rostral pole of the MAOr and motor and posterior parietal cortices to its caudal parts (section "Nuclei at the Mesodiencephalic Border: The Central and Medial Tegmental Tracts" and Fig. 19.13). The rostral pole of the MAOr projects to the flocculus and the adjacent ventral paraflocculus. The dorsal paraflocculus and the ansiform lobule receive their climbing fibers from successively more caudal parts of the MAOr. The caudal portion of the MAOr, which receives motor and parietal input, projects to the C2 zone of the anterior lobe and the paramedian lobule (Brodal and Kawamura 1980). Laterocaudal visuomotor and rostromedial skeletomotor divisions also have been recognized in the posterior interposed nucleus (van Kan et al. 1993). The laterocaudal visuomotor division receives a corticonuclear projection from the paraflocculus (Xiong and Nagao 2002). The topical projections of the more rostral segments of the C2 zone to the posterior interposed nucleus have not yet been studied.

Efferent connections of the posterior interposed nucleus (Fig. 19.32a) include the contralateral magnocellular red nucleus, Darkschewitsch' nucleus, the near-response region located dorsal to the oculomotor nuclei which is required for vergence eye movements (May et al. 1992), the superior colliculus and, as thalamocortical projections, the primary motor and premotor cortex and the frontal eye fields and posterior parietal areas (Kievit 1979; Lynch and Tian 2006; Matelli

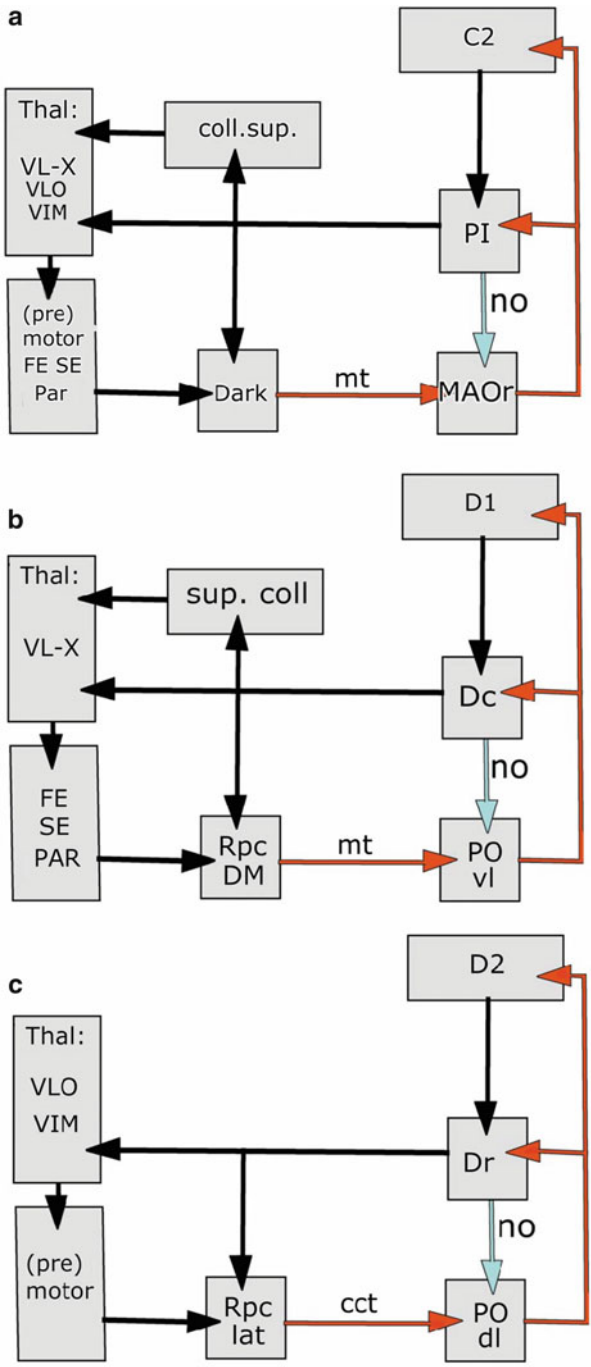

Fig. 19.32 Diagrams of the projections of the posterior interposed nucleus (**a**), the caudal dentate nucleus (**b**), and the rostral dentate nucleus (**c**). Recurrent climbing fiber pathways are indicated in *red*. Abbreviations: *ctt* central tegmental tract, *coll.sup* superior colliculus, *Dark* Darkschewitsch' nucleus, *Dc* caudal dentate nucleus, *Dr* rostral dentate nucleus, *FA* supplementary eye field, *FE* frontal eye field, *MAOr* rostral medial accessory olive, *mt* medial tegmental tract, *no* nucleo-olivary pathway, *Par* parietal cortex, *PI* posterior interposed nucleus, *POdl* dorsal lamina principal olive, *POvl* ventral lamina principal olive, *Rpc DM* dorsomedial subdivision parvocellular red nucleus (Bechterew's nucleus), *Rpc lat* lateral subdivision parvocellular red nucleus, *Thal* thalamus, *VIM* ventral intermediate thalamic nucleus, *VLO* ventral lateral thalamic nucleus oral part, *VL-X* ventral lateral thalamic nucleus, nucleus X

and Luppino 1996; Matelli et al. 1989). Another link with the frontal eye field and, possibly, parietal areas is provided by the superior colliculus (Lynch et al. 1994; Tian and Lynch 1997). Extensive projections to the medial intraparietal area MIP, from the anterior and paramedian C2 zone, through the laterocaudal half of the posterior interposed nucleus and a more restricted projection of its laterocaudal pole to the ventral lateral intraparietal area LIP were documented by Prevosto et al. (2009). Efferents of the posterior interposed nucleus largely overlap with those from the anterior interposed and dentate nuclei. Darkschewitsch nucleus constitutes the link in the direct and indirect reciprocal climbing fiber paths (Fig. 19.32a).

The interstitial cell groups share projections to the vestibular nuclei, the reticular formation, the red nucleus, and the thalamus with neighboring nuclei (Buisseret-Delmas et al. 1998; Teune et al. 2000). A specific feature of this cell group is its collateral projection to the spinal cord with the caudal medial reticular formation and to the thalamus with the superior colliculus (Bentivoglio and Kuypers 1982).

Dentate Nucleus

The dentate nucleus can be divided into rostrodorsal and caudoventral parts that receive corticonuclear projections of the D1 and D2 zones, respectively, and collaterals from the olivocerebellar fibers that innervate these two zones (Fig. 19.18). Rostral motor and ventrocaudal non-motor divisions were distinguished by Strick in the cebus monkey (Strick et al. 2009). A visuomotor division was identified in the ventrocaudal pole of the monkey dentate (van Kan et al. 1993). It is not known whether these different modes that partition the dentate nucleus define the same rostrocaudal subdivisions.

The caudal visuomotor division of the dentate nucleus gives rise to a component of the brachium conjunctivum that terminates contralaterally in the dorsomedial parvocellular red nucleus, the superior colliculus and medially in the ventrolateral thalamic nucleus including area X, with minor extensions in the adjoining mediodorsal and anterior nuclei (Fig. 19.32b). The rostral dentate projects to the lateral and caudal parvocellular red nucleus and the ventral intermediate and lateral portions of the ventral lateral thalamic nucleus (Chan-Palay 1977; Kievit 1979) (Fig. 19.29c). Nucleo-olivary pathways connect the rostral dentate with the dorsal lamina and the lateral bend of the inferior olive, and the caudal dentate with the ventral lamina (section "The Nucleo-olivary Pathway").

Strick's distinction in the monkey dentate of rostrodorsal motor and ventrocaudal non-motor divisions is based on retrograde transneuronal labeling experiments. Neurons in the motor division can be labeled from the primary and premotor cortex including the supplementary motor area (SMA). Neurons in the caudal non-motor division are connected with the preSMA and the prefrontal areas 9d and 46 (Fig. 19.33). A projection to the frontal eye field was located in the

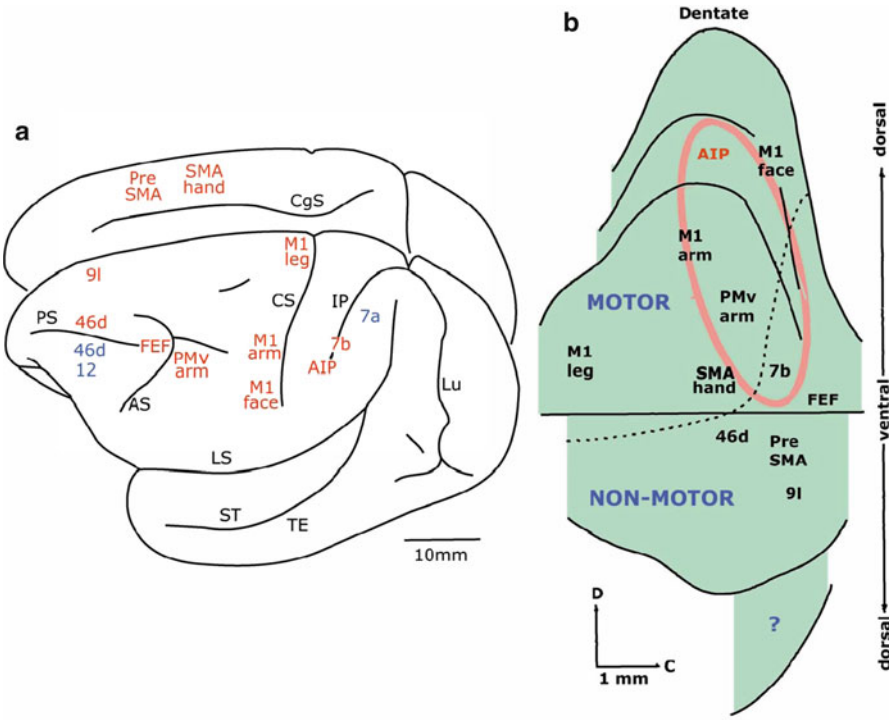

Fig. 19.33 Diagram illustrating transneuronal retrograde labeling from injection sites in different cortical areas in the cebus monkey. (**a**) Localization of injection sites resulting in labeling within the dentate nucleus (*red*) and in cases without labeling of this nucleus (*blue*). (**b**) Diagram of the unfolded dentate nucleus of the cebus monkey, showing approximate position of the labeling from injections of different cortical areas. *Broken line* indicates border between motor and non-motor divisions of the dentate nucleus. *Question mark* indicated the non-explored medial lamina of the dentate nucleus. *Red ellipse* indicates extent of the labeling from an injection of the anterior intraparietal area that includes both the motor and non-motor divisions of the nucleus (Reproduced and modified from Strick et al. (2009)). Abbreviations: *IP* anterior intraparietal area, *AS* arcuate sulcus, *CgS* cingulate sulcus, *CS* central sulcus, *FEF* frontal eye field, *PS* principal sulcus, *IP* intraparietal sulcus, *LS* lateral sulcus, *Lu* lunate sulcus, *M1* primary motor cortex, *PMv* ventral premotor area, *PreSMA* rostral division of the supplementary motor area, *SMA* supplementary motor area (SMA proper), *ST* superior, *TE* temporal lobe, *ST* temporal sulcus

extreme caudal pole of the nucleus (Strick et al. 2009) (Fig. 19.32b, c). Neurons projecting to the anterior intraparietal area (AIP; Clower et al. 2005) are located in both the motor and non-motor divisions, and those projecting to the medial intraparietal (MIP) mainly occupy the rostral dentate (Prevosto et al. 2009). Projections to parietal area 7b (Clower et al. 2001) and the lateral intraparietal area (LIP; Prevosto et al. 2009) are derived from its non-motor division.

The dorsomedial parvocellular red nucleus, the medial tegmental tract, and the ventral lamina of the principal olive are links in direct and indirect recurrent projections from the frontal eye fields and parietal areas to the caudal dentate and the D1 zone. The lateral and caudal parvocellular red nucleus, the central tegmental tract, and the dorsal lamina of the principal olive are links in the recurrent pathway from motor and premotor cortical areas to the rostral dentate and the D2 zone (Figs. 19.14 and 19.32b, c).

The zonal organization of the connections of the inferior olive and the cerebellar nuclei, as described in this chapter, adequately covers the anatomy of the cerebellum of lower mammals. However, our knowledge of the connections of the hemisphere of the great apes and the human cerebellum, which accounts for the bulk of the cerebellar cortex in these species, remains incomplete. The demonstration by Fujita et al. (2010) of the presence of D1 and D2 zones in the marmoset hemisphere does support the idea that the construction of the primate hemisphere is similar to that in rodents and carnivores, but the relative proportions of the marmoset hemisphere are not very different from rodents. The source of the climbing fiber projection to the D1 zone in rodents and primates is the ventral, non-convoluted lamina of the principal olive (section "The Corticonuclear and Olivocerebellar Projections"). If this subdivision of the principal olive is represented in the human inferior olive by its medial lamina (Fig. 19.3), the contribution of the human D1 zone to the hemisphere would be small indeed. Its major output would be represented by the D2 zone, with its projection to the convoluted dentate nucleus. In this case, the subdivision of the human dentate in rostrodorsal microgyric and caudolateral macrogyric portions would correspond with two major subdivisions of the D2 zone. There is no evidence on the corticonuclear projection of the human cerebellar hemisphere. The only observations on the connections of the two parts of the human dentate stem from papers on crossed cerebro-cerebellar atrophy by Demolé (1927a, b) and Verhaart and Wieringen-Rauws (1950). Demolé concluded that degeneration of the rostrodorsal, microgyric dentate occurred with large, chronic lesions involving the pre- and postcentral gyri. Lesions of more posterior parts of the hemisphere, involving parietal, occipital, and temporal areas, resulted in atrophy of the ventrocaudal macrogyric dentate. Prefrontal lesions would spare the dentate nucleus. These observations still need to be confirmed but, at least, emphasize the possibility that the increase in size of the cerebellar hemisphere is also related to the elaboration of its connections with postrolandic areas, in addition to the expansion of the cerebello-prefrontal connectivity, as advocated by many cognitive neuroscientists. Interestingly, Masao Ito (2012) in his recent book "*The cerebellum. Brain for an Implicit Self*" proposes a neural control system for mental activities that includes both prefrontal and postrolandic areas and the cerebellar hemispheres. In this system, the prefrontal cortex serves as the controller, the representation of the controlled subjects is found in the temporoparietal cortex, and the cerebellar hemispheres provide the internal models of the controlled objects represented in the temporoparietal cortex.

References

Ackerley R, Pardoe J, Apps R (2006) A novel site of synaptic relay for climbing fibre pathways relaying signals from the motor cortex to the cerebellar cortical C1 zone. J Physiol 57:503–518

Akaike T (1989) Electrophysiological analysis of the trigemino-olivo-cerebellar (crura I and II, lobulus simplex) projection in the rat. Brain Res 20:402–406

Akaike T (1992) The tectorecipient zone in the inferior olivary nucleus in the rat. J Comp Neurol 320:398–414

Alonso A, Blanco MJ, Paino CL, Rubia FJ (1986) Distribution of neurons in the main cuneate nucleus projecting to the inferior olive in the cat. Evidence that they differ from those directly projecting to the cerebellum. Neuroscience 18:671–683

Andersson G (1984) Demonstration of a cuneate relay in a cortico-olivo-cerebellar pathway in the cat. Neurosci Lett 46:47–52

Andersson G, Eriksson L (1981) Spinal, trigeminal, and cortical climbing fibre paths to the lateral vermis of the cerebellar anterior lobe in the cat. Exp Brain Res 44:71–81

Andersson G, Oscarsson O (1978) Climbing fiber microzones in cerebellar vermis and their projection to different groups of cells in the lateral vestibular nucleus. Exp Brain Res 32:565–579

Angaut P, Brodal A (1967) The projection of the "vestibulocerebellum" onto the vestibular nuclei in the cat. Arch Ital Biol 105:441–479

Armstrong DM, Schild RF (1979) Spino-olivary neurones in the lumbo-sacral cord of the cat demonstrated by retrograde transport of horseradish peroxidase. Brain Res 168:176–179

Armstrong DM, Harvey RJ, Schild RF (1973) Branching of inferior olivary axons to terminate in different folia, lobules or lobes of the cerebellum. Brain Res 54:365–371

Armstrong DM, Campbell MC, Edglet SA, Schild RF (1982) Investigations of the olivocerebellar and spino-olivary pathways. Exp Brain Res 6:195–232

Azizi SA, Woodward DJ (1987) Inferior olivary nuclear complex of the rat: morphology and comments on the principles of organization within the olivocerebellar system. J Comp Neurol 263:467–484

Bagnall MW, Zingg B, Sakatos A, Moghadam SH, Zeilhofer HU, du Lac S (2009) Glycinergic projection neurons of the cerebellum. J Neurosci 29:10104–10110

Barmack NH (2006) Inferior olive and oculomotor system. Prog Brain Res 151:269–291

Barmack NH, Fagerson M, Errico P (1993) Cholinergic projection to the dorsal cap of the inferior olive of the rat, rabbit, and monkey. J Comp Neurol 328:263–281

Barmack NH, Fredette BJ, Mugnaini E (1998) Parasolitary nucleus: a source of GABAergic vestibular information to the inferior olive of rat and rabbit. J Comp Neurol 392:352–372

Batton RR 3rd, Jayaraman A, Ruggiero D, Carpenter MB (1977) Fastigial efferent projections in the monkey: an autoradiographic study. J Comp Neurol 174:281–305

Beitz AJ (1976) The topographical organization of the olivo-dentate and dentato-olivary pathways in the cat. Brain Res 115:311–317

Bentivoglio M, Kuypers HGJM (1982) Divergent axon collaterals from rat cerebellar nuclei to diencephalon, mesencephalon, medulla oblongata and cervical cord. Exp Brain Res 46:339–356

Berkley KJ, Hand PJ (1978) Projections to the inferior olive of the cat. II. Comparisons of input from the gracile, cuneate and the spinal trigeminal nuclei. J Comp Neurol 180:253–264

Bertrand I, Marechal P (1930) Étude morphologique du complexe olivaire inférieur chez l'homme. Revue Neurol 53:705–736

Bigaré F (1980) De efferente verbindingen van de cerebellaire schors van de kat. Thesis, Leiden University

Boesten AJ, Voogd J (1975) Projections of the dorsal column nuclei and the spinal cord on the inferior olive in the cat. J Comp Neurol 161:215–237

Borra E, Belmalih A, Gerbella M, Rozzi S, Luppino G (2010) Projections of the hand field of the macaque ventral premotor area F5 to the brainstem and spinal cord. J Comp Neurol 518:2570–2591

Bowman JP, Sladek JR Jr (1973) Morphology of the inferior olivary complex of the rhesus monkey (*Macaca mulatta*). J Comp Neurol 152:299–316
Brodal A (1940) Untersuchungen über die Olivocerebellaren Lokalisation. Z Neurol 169:1053
Brodal P, Brodal A (1981) The olivocerebellar projection in the monkey. Experimental studies with the method of retrograde tracing of horseradish peroxidase. J Comp Neurol 201:375–393
Brodal A, Kawamura K (1980) Olivocerebellar projection: a review. Adv Anat Embryol Cell Biol 64:1–137
Brodal A, Walberg F, Blackstad T (1950) Termination of spinal afferents to inferior olive in cat. J Neurophysiol 13:431–454
Brown JT, Chan-Palay V, Palay SL (1977) A study of afferent input to the inferior olivary complex in the rat by retrograde axonal transport of horseradish peroxidase. J Comp Neurol 176:1–22
Buisseret-Delmas C (1982) An HRP study of the afferents to the inferior olive in cat. Arch Ital Biol 118:270–286
Buisseret-Delmas C (1988) Sagittal organization of the olivocerebellonuclear pathway in the rat. I. Connections with the nucleus fastigii and the nucleus vestibularis lateralis. Neurosci Res 5:475–493
Buisseret-Delmas C (1989) Sagittal organization of the olivocerebellonuclear pathway in the rat. III. Connections with the nucleus dentatus. Neurosci Res 7:131–143
Buisseret-Delmas C, Angaut P (1993) The cerebellar olivo-corticonuclear connections in the rat. Prog Neurobiol 40:63–87
Buisseret-Delmas C, Angaut P, Compoint C, Diagne M, Buisseret P (1998) Brainstem efferents from the interface between the nucleus medialis and the nucleus interpositus in the rat. J Comp Neurol 402:264–275
Bull MS, Mitchell SK, Berkley KJ (1990) Convergent inputs to the inferior olive from the dorsal column nuclei and pretectum in the cat. Brain Res 525:1–10
Burman K, Darian-Smith C, Darian-Smith I (2000) Macaque red nucleus: origins of spinal and olivary projections and terminations of cortical inputs. J Comp Neurol 423:179–196
Cajal SRy (1972) Histologie du système nerveux de l'homme et des vertebrés, vol 2. Consejo Superior de Investigaciones Cientificas, Madrid
Campbell NC, Armstrong DM (1985) Origin in the medial accessory olive of climbing fibres to the x and lateral c1 zones of the cat cerebellum: a combined electrophysiological/WGA-HRP investigation. Exp Brain Res 58:520–531
Catsman-Berrevoets CE, Kuypers HJGM, Lemon RN (1979) Cells of origin of the cortical projections to magnocellular and parvocellular red nucleus and superior colliculus in cynomolgus monkey. An HRP study. Neurosci Lett 12:41–46
Chan-Palay V (1977) Cerebellar dentate nucleus: organization, cytology and transmitters. Springer, Berlin
Chen S, Hillman DE (1993) Colocalization of neurotransmitters in the deep cerebellar nuclei. J Neurocytol 22:81–91
Clower DM, West RA, Lynch JC, Strick PL (2001) The inferior parietal lobule is the target of output from the superior colliculus, hippocampus, and cerebellum. J Neurosci 21:6283–6291
Clower DM, Dum RP, Strick PL (2005) Basal ganglia and cerebellar inputs to 'AIP'. Cereb Cortex 15(7):913–920
Cook JR, Wiesendanger M (1976) Input from trigeminal cutaneous afferents to neurones of the inferior olive in rats. Exp Brain Res 26:193–202
Courville J (1975) Distribution of olivocerebellar fibers demonstrated by a radioautographic method. Brain Res 95:253–263
Courville J, Cooper CW (1970) The cerebellar nuclei of *Macaca mulatta*: a morphological study. J Comp Neurol 140:241–254
Courville J, Faraco-Cantin F (1978) On the origin of the climbing fibers of the cerebellum. An experimental study in the cat with an autoradiographic tracing method. Neuroscience 3:797–809
Courville J, Faraco-Cantin F, Diakiw N (1974) A functionally important feature of the distribution of the olivo-cerebellar climbing fibers. Can J Physiol Pharmacol 52:1212–1217

Courville J, Faraco-Cantin F, Legendre A (1983a) Detailed organization of cerebello-olivary projections in the cat. An autoradiographic study. Arch Ital Biol 121:219–236
Courville J, Faraco-Cantin F, Marcon L (1983b) Projections from the reticular formation of the medulla, the spinal trigeminal and lateral reticular nuclei to the inferior olive. Neuroscience 9:129–139
De Zeeuw CI, Wentzel P, Mugnaini E (1993) Fine structure of the dorsal cap of the inferior olive and its GABAergic and non-GABAergic input from the nucleus prepositus hypoglossi in rat and rabbit. J Comp Neurol 327:63–82
De Zeeuw CI, Gerrits NM, Voogd J, Leonard CS, Simpson JI (1994a) The rostral dorsal cap and ventrolateral outgrowth of the rabbit inferior olive receive a GABAergic input from dorsal group Y and the ventral dentate nucleus. J Comp Neurol 341:420–432
De Zeeuw CI, Wylie DR, DiGiorgi PL, Simpson JI (1994b) Projections of individual Purkinje cells of identified zones in the flocculus to the vestibular and cerebellar nuclei in the rabbit. J Comp Neurol 349:428–447
Demolé V (1927a) Structure et cnnexions des noyeaux denreles du cervelet. I. Schweiz Arch Neurol Psychiat 20:271–294
Demolé V (1927b) Structure et connection des noyeaux denteles du cervelet. II. Schweiz Arch Neurol u Psychiat 21:73–1110
Desclin JC (1974) Histological evidence supporting the inferior olive as the major source of cerebellar climbing fibers in the rat. Brain Res 77:365–384
Eccles JC, Llinas R, Sasaki K (1966) The excitatory synaptic action of climbing fibres on the Purkinje cells of the cerebellum. J Physiol 182:268–296
Ekerot CF, Larson B (1979a) The dorsal spino-olivocerebellar system in the cat. I. Functional organization and termination in the anterior lobe. Exp Brain Res 36(2):201–217
Ekerot CF, Larson B (1979b) The dorsal spino-olivocerebellar system in the cat. II. Somatotopical organization. Exp Brain Res 36:219–232
Ekerot CF, Larson B (1982) Branching of olivary axons to innervate pairs of sagittal zones in the cerebellar anterior lobe of the cat. Exp Brain Res 48:185–198
Ekerot CF, Garwicz M, Schouenborg J (1991) The postsynaptic dorsal column pathway mediates cutaneous nociceptive information to cerebellar climbing fibres in the cat. J Physiol 441: 275–284
Faugier-Grimaud S, Ventre J (1989) Anatomic connections of inferior parietal cortex (area 7) with subcortical structures related to vestibulo-ocular function in a monkey (*Macaca fascicularis*). J Comp Neurol 280:1–14
Frankfurter A, Weber JT, Royce GJ, Strominger NL, Harting JK (1976) An autoradiographic analysis of the tecto-olivary projection in primates. Brain Res 118:245–257
Fujita H, Oh-Nishi A, Obayashi S, Sugihara I (2010) Organization of the marmoset cerebellum in three-dimensional space: lobulation, aldolase C compartmentalization and axonal projection. J Comp Neurol 518:1764–1791
Garwicz M (1997) Sagittal zonal organization of climbing fiber input to the cerebellar anterior lobe of the ferret. Exp Brain Res 117:389–398
Garwicz M, Ekerot CF (1994) Topographical organization of the cerebellar cortical projection to nucleus interpositus anterior in the cat. J Physiol 474:245–260
Garwicz M, Ekerot CF, Schouenborg J (1992) Distribution of cutaneous nociceptive and tactile climbing fibre input to sagittal zones in cat cerebellar anterior lobe. Eur J Neurosci 4: 289–295
Gellman R, Houk JC, Gibson AR (1983) Somatosensory properties of the inferior olive of the cat. J Comp Neurol 215:228–243
Gerrits NM, Voogd J (1982) The climbing fiber projection to the flocculus and adjacent paraflocculus in the cat. Neuroscience 7:2971–2991
Gerrits NM, Voogd J (1986) The nucleus reticularis tegmenti pontis and the adjacent rostral paramedian reticular formation: differential projections to the cerebellum and the caudal brain stem. Exp Brain Res 62:29–45

Gerrits NM, Voogd J, Magras IN (1985) Vestibular afferents of the inferior olive and the vestibulo-olivo-cerebellar climbing fiber pathway to the flocculus in the cat. Brain Res 332(2):325–336
Gibson AR, Horn KM, Pong M (2002) Inhibitory control of olivary discharge. Ann NY Acad Sci 978:219–231
Giolli RA, Blanks RH, Lui F (2006) The accessory optic system: basic organization with an update on connectivity, neurochemistry, and function. Prog Brain Res 151:407–440
Glickstein M, Strata P, Voogd J (2009) Cerebellum: history. Neuroscience 162:549–559
Goodman DC, Hallett RE, Welch RB (1963) Patterns of localization in the cerebellar corticonuclear projections of the albino rat. J Comp Neurol 121:51–67
Graybiel AM, Hartwieg EA (1974) Some afferent connections of the oculomotor complex in the cat: an experimental study with tracer techniques. Brain Res 81:543–551
Graybiel AM, Nauta HJ, Lasek RJ, Nauta WJ (1973) A cerebello-olivary pathway in the cat: an experimental study using autoradiographic tracing techniques. Brain Res 58:205–211
Groenewegen HJ, Voogd J (1977) The parasagittal zonation within the olivocerebellar projection. I. Climbing fiber distribution in the vermis of cat cerebellum. J Comp Neurol 174:417–488
Groenewegen HJ, Boesten AJ, Voogd J (1975) The dorsal column nuclear projections to the nucleus ventralis posterior lateralis thalami and the inferior olive in the cat: an autoradiographic study. J Comp Neurol 162:505–517
Groenewegen HJ, Voogd J, Freedman SL (1979) The parasagittal zonation within the olivocerebellar projection. II. Climbing fiber distribution in the intermediate and hemispheric parts of cat cerebellum. J Comp Neurol 183:551–601
Haines DE (1977) Cerebellar corticonuclear and corticiovetibular fibers of the flocculonodular lobe in a prosimian primate (*Galago senegalensis*). J Comp Neurol 174:607–630
Haines DE, Patrick GW, Satrulee P (1982) Organization of cerebellar corticonuclear fiber systems. Exp Brain Res 6:320–371
Harting JK (1977) Descending pathways from the superior colliculus: an autoradiographic analysis in the rhesus monkey (*Macaca mulatta*). J Comp Neurol 173:583–612
Hawkes R, Herrup K (1995) Aldolase C/zebrin II and the regionalization of the cerebellum. J Mol Neurosci 6:147–158
Hawkes R, Leclerc N (1986) Immunocytochemical demonstration of topographic ordering of Purkinje cell axon terminals in the fastigial nucleus of the rat. J Comp Neurol 244:481–491
Hawkes R, Leclerc N (1987) Antigenic map of the rat cerebellar cortex: the distribution of parasagittal bands as revealed by monoclonal anti-Purkinje cell antibody mapQ113. J Comp Neurol 256:29–41
Hess DT (1982) The tecto-olivo-cerebellar pathway in the rat. Brain Res 250:143–148
Hess DT, Voogd J (1986) Chemoarchitectonic zonation of the monkey cerebellum. Brain Res 369:383–387
Holmes G, Steward TG (1908) On the connections of the inferior olives with the cerebellum in man. Brain 31:125–137
Holstege G, Collewijn H (1982) The efferent connections of the nucleus of the optic tract and the superior colliculus in the rabbit. J Comp Neurol 209:139–175
Homma Y, Nonaka S, Matsuyama K, Mori S (1995) Fastigiofugal projection to the brainstem nuclei in the cat: an anterograde PHA-L tracing study. Neurosci Res 23:89–102
Huerta MF, Harting JK (1984) Connectional organization of the superior colliculus. Trends Neurosci 7:286–289
Huerta MF, Kaas H (1990) Supplementary eye field as defined by intracortical microstimulation: connections in macaques. J Comp Neurol 293:299–330
Huerta MF, Frankfurter A, Harting JK (1983) Studies of the principal sensory and spinal trigeminal nuclei of the rat: projections to the superior colliculus, inferior olive and cerebellum. J Comp Neurol 220:147–167
Huerta MF, Krubitzer LA, Kaas JH (1986) Frontal eye field as defined by intracortical microstimulation in squirrel monkeys, owl monkeys, and macaque monkeys: I. Subcortical connections. J Comp Neurol 253:415–439

Huisman AM, Kuypers HG, Conde F, Keizer K (1983) Collaterals of rubrospinal neurons to the cerebellum in rat. A retrograde fluorescent double labeling study. Brain Res 264:181–196

Humphrey DR, Gold R, Reed DJ (1984) Sites, laminar and topographical origins of cortical projections to the major divisions of the red nucleus in the monkey. J Comp Neurol 225:75–94

Ito M (2012) The cerebellum. Brain for an implicit self. FT Press, Upper Saddle River

Itoh K, Takada M, Yasui Y, Kudo M, Mizuno N (1983) Direct projections from the anterior pretectal nucleus to the dorsal accessory olive in the cat: an anterograde and retrograde WGA-HRP study. Brain Res 272:350–353

Jansen J, Brodal A (1940) Experimental studies on the intrinsic fibers of the cerebellum. II. The corticonuclear projection. J Comp Neurol 73:267–321

Jansen J, Brodal A (1942) Experimental studies on the intrinsic fibers of the cerebellum. III. Cortico-nuclear projection in the rabbit and the monkey. Norsk Vid Akad Avh 1 Math Nat Kl 3:1–50

Jürgens U (1984) The efferent and afferent connections of the supplementary motor area. Brain Res 300:63–81

Kalil K (1979) Projections of the cerebellar and dorsal column nuclei upon the inferior olive in the rhesus monkey: an autoradiographic study. J Comp Neurol 188:43–62

Kawamura K, Onodera S (1984) Olivary projections from the pretectal region in the cat studied with horseradish peroxidase and tritiated amino acids axonal transport. Arch Ital Biol 122: 155–168

Kawamura S, Hattori S, Higo S, Matsuyama T (1982) The cerebellar projections to the superior colliculus and pretectum in the cat: an autoradiographic and horseradish peroxidase study. Neuroscience 7:1673–1689

Kievit J (1979) Cerebello-thalamische projecties en de afferente verbindingen naar de frontaalschors in de rhesusaap. Thesis, Erasmus University, Rotterdam

King JS, Martin GF, Bowman MH (1975) The direct spinal area of the inferior olivary nucleus: an electron microscopic study. Exp Brain Res 22:13–24

Kitao Y, Nakamura Y, Kudo M, Moriizumi T, Tokuno H (1989) The cerebral and cerebellar connections of pretecto-thalamic and pretecto-olivary neurons in the anterior pretectal nucleus of the cat. Brain Res 484:304–313

Kooy FH (1917) The inferior olive in vertebrates. Folia Neurobiol 10:205–369

Kuypers HG, Lawrence DG (1967) Cortical projections to the red nucleus and the brain stem in the rhesus monkey. Brain Res 4(2):151–188

Langer T, Fuchs AF, Scudder CA, Chubb MC (1985) Afferents to the flocculus of the cerebellum in the rhesus macaque as revealed by retrograde transport of horseradish peroxidase. J Comp Neurol 235:1–25

Legendre A, Courville J (1986) Cerebellar nucleocortical projection with a survey of factors affecting the transport of radioactive tracers. J Comp Neurol 252:392–403

Leichnetz GR (1982) The medial accessory nucleus of Bechterew: a cell group within the anatomical limits of the rostral oculomotor complex receives a direct prefrontal projection in the monkey. J Comp Neurol 210:147–151

Leichnetz GR (2001) Connections of the medial posterior parietal cortex (area 7 m) in the monkey. Anat Rec 263:215–236

Leichnetz GR, Gonzalo-Ruiz A (1996) Prearcuate cortex in the cebus monkey has cortical and subcortical connections like the macaque frontal eye field and projects to fastigial-recipient oculomotor-related brainstem nuclei. Brain Res Bull 41:1–29

Leichnetz GR, Spencer RF, Smith DJ (1984) Cortical projections to nuclei adjacent to the oculomotor complex in the medial dien-mesencephalic tegmentum in the monkey. J Comp Neurol 228:359–387

Leto K, Carletti B, Williams IM, Magrassi L, Rossi F (2006) Different types of cerebellar GABAergic interneurons originate from a common pool of multipotent progenitor cells. J Neurosci 26:11682–11694

Loewy AD, Burton H (1978) Nuclei of the solitary tract: efferent projections to the lower brain stem and spinal cord of the cat. J Comp Neurol 181:421–449
Lynch JC, Tian JR (2006) Cortico-cortical networks and cortico-subcortical loops for the higher control of eye movements. Prog Brain Res 151:461–501
Lynch JC, Hoover JE, Strick PL (1994) Input to the primate frontal eye field from the substantia nigra, superior colliculus, and dentate nucleus demonstrated by transneuronal transport. Exp Brain Res 100:181–186
Marechal P (1934) L'olive bulbaire. Anatomie, ontogénèse, phylogenèse, physiologie et physiopathologie. Doin et Cie, Paris
Marr D (1969) A theory of cerebellar cortex. J Physiol 202:437–470
Martin GF, Culberson J, Laxson C, Linauts M, Panneton M, Tschimadia I (1980) Afferent connexions of the inferior olivary nucleus with preliminary notes on their development: studies using the North American opossum. In: Courville J, De Montigny C, Lamarre Y (eds) The inferior olivary nucleus. Raven, New York
Matelli M, Luppino G (1996) Thalamic input to mesial and superior area 6 in the macaque monkey. J Comp Neurol 372:59–87
Matelli M, Luppino G, Fogassi L, Rizzolatti G (1989) Thalamic input to inferior area 6 and area 4 in the macaque monkey. J Comp Neurol 280:468–488
May PJ, Hartwich-Young R, Nelson J, Sparks DL, Porter JD (1990) Cerebellotectal pathways in the macaque: implications for collicular generation of saccades. Neuroscience 36(2):305–324
May PJ, Porter JD, Gamlin PD (1992) Interconnections between the primate cerebellum and midbrain near-response regions. J Comp Neurol 315(1):98–116
McCrea RA, Baker R (1985) Anatomical connections of the nucleus prepositus of the cat. J Comp Neurol 237:377–407
McCrea RA, Bishop GA, Kitai ST (1978) Morphological and electrophysiological characteristics of projection neurons in the nucleus interpositus of the cat cerebellum. J Comp Neurol 181:397–419
McCurdy ML, Gibson AR, Houk JC (1992) Spatial overlap of rubrospinal and corticospinal terminals with input to the inferior olive. Neuroimage 1:23–41
Mehler WR (1969) Some neurological species differences:a posteriori. Ann NY Acad Sci 167:424–468
Miyashita E, Tamai Y (1989) Subcortical connections of frontal 'oculomotor' areas in the cat. Brain Res 502:75–87
Mizuno N (1966) An experimental study of the spino-olivary fibers in the rabbit and the cat. J Comp Neurol 127:267–292
Molinari HH (1984) Ascending somatosensory projections to the dorsal accessory olive: an anatomical study in cats. J Comp Neurol 223:110–123
Molinari HH (1985) Ascending somatosensory projections to the medial accessory portion of the inferior olive: a retrograde study in cats. J Comp Neurol 232:523–533
Molinari HH, Starr KA (1989) Spino-olivary termination on spines in cat medial accessory olive. J Comp Neurol 288:254–262
Molinari HH, Starr KA, Sluyters RN (1991) Gracile projection to the cat medial accessory olive: ultrastructural termination patterns and convergence with spino-olivary projection. J Comp Neurol 309:363–374
Molinari HH, Schultze KE, Strominger NL (1996) Gracile, cuneate, and spinal trigeminal projections to inferior olive in rat and monkey. J Comp Neurol 375:467–480
Mugnaini E, Oertel WH (1985) GABAergic neurons and terminals in rat CNS as revealed by GAD immuno-histochemistry. In: Björklund A, Hokfelt T (eds) GABA and neuropeptides in the CNS: the handbook of chemical neuroanatomy, Part 1, vol 4. Elsevier, Amsterdam
Nakamura Y, Kitao Y, Okoyama S (1983) Projections from the pericruciate cortex to the nucleus of Darkschewitsch and other structures at the mesodiencephalic junction in the cat. Brain Res Bull 10:517–521
Nelson BJ, Mugnaini E (1989) Origin of GABAergic inputs to the inferior olive. Exp Brain Res Ser 17:86–107

Noda H, Sugita S, Ikeda Y (1990) Afferent and efferent connections of the oculomotor region of the fastigial nucleus in the macaque monkey. J Comp Neurol 302:330–348

Ogawa T (1935) Beiträge zur vergleichende Anatomie des Zentralnervensystems der Wassersäugetiere. Ueber die Kleinhirnkerne der Pinnipedien und Cetaceen. Arb Anat Inst Sendai 17:63–136

Ogawa T (1939) The tractus tegmenti medialis and its connection with the inferior olive in the cat. J Comp Neurol 70:181–190

Oka H (1988) Functional organization of the parvocellular red nucleus in the cat. Behav Brain Res 28:233–240

Onodera S (1984) Olivary projections from the mesodiencephalic structures in the cat studied by means of axonal transport of horseradish peroxidase and tritiated amino acids. J Comp Neurol 227:37–49

Orioli PJ, Strick PL (1989) Cerebellar connections with the motor cortex and the arcuate premotor area: an analysis employing retrograde transneuronal transport of WGA-HRP. J Comp Neurol 288:612–626

Oscarsson O (1969) Termination and functional organization of the dorsal spino-olivocerebellar path. J Physiol 200:129–149

Oscarsson O, Sjölund B (1977a) The ventral spine-olivocerebellar system in the cat. II. Termination zones in the cerebellar posterior lobe. Exp Brain Res 28:487–503

Oscarsson O, Sjölund B (1977b) The ventral spino-olivocerebellar system in the cat. I. Identification of five paths and their termination in the cerebellar anterior lobe. Exp Brain Res 28:469–486

Oscarsson O, Sjölund B (1977c) The ventral spino-olivocerebellar system in the cat. III. Functional characteristics of the five paths. Exp Brain Res 28:505–520

Oscarsson O, Uddenberg N (1966) Somatotopic termination of spino-olivocerebellar path. Brain Res 3:204–207

Pijpers A, Voogd J, Ruigrok TJ (2005) Topography of olivo-cortico-nuclear modules in the intermediate cerebellum of the rat. J Comp Neurol 492:193–213

Porter CM, Van Kan PLE, Horn KM, Bloedel JR, Gibson AR (1993) Functional divisions of cat rMAO. Abstr Soc Neurosci 19:499–510

Prevosto V, Graf W, Ugolini G (2009) Cerebellar inputs to intraparietal cortex areas LIP and MIP: functional frameworks for adaptive control of eye movements, reaching, and arm/eye/head movement coordination. Cereb Cortex 20:214–228

Probst M (1901) Zur Kenntniss des Beinderams, der Haubenstrahlung und des Regio Subthalamica. Mschr f Psychiat u Neurol 35:692–777

Rexed B (1952) The cytoarchitectonic organization of the spinal cord in the cat. J Comp Neurol 96:441–495

Richmond FJ, Courville J, Saint-Cyr JA (1982) Spino-olivary projections from the upper cervical spinal cord: an experimental study using autoradiography and horseradish peroxidase. Exp Brain Res 47:239–251

Ruigrok TJ (2003) Collateralization of climbing and mossy fibers projecting to the nodulus and flocculus of the rat cerebellum. J Comp Neurol 466:278–298

Ruigrok TJ (2004) Precerebellar nuclei and red nucleus. In: Paxinos G (ed) The rat nervous system, 3rd edn. Elsevier, Amsterdam, pp 167–204

Ruigrok TJ, Voogd J (1990) Cerebellar nucleo-olivary projections in the rat: an anterograde tracing study with *Phaseolus vulgaris*-leucoagglutinin (PHA-L). J Comp Neurol 298:315–333

Ruigrok TJ, Voogd J (2000) Organization of projections from the inferior olive to the cerebellar nuclei in the rat. J Comp Neurol 426:209–228

Ruigrok TJ, Osse RJ, Voogd J (1992) Organization of inferior olivary projections to the flocculus and ventral paraflocculus of the rat cerebellum. J Comp Neurol 316:129–150

Saint-Cyr JA (1983) The projection from the motor cortex to the inferior olive in the cat. An experimental study using axonal transport techniques. Neuroscience 10:667–684

Saint-Cyr JA (1987) Anatomical organization of cortico-mesencephalo-olivary pathways in the cat as demonstrated by axonal transport techniques. J Comp Neurol 257:39–59
Saint-Cyr JA, Courville J (1979) Projection from the vestibular nuclei to the inferior olive in the cat: an autoradiographic and horseradish peroxidase study. Brain Res 165:189–200
Saint-Cyr JA, Courville J (1982) Descending projections to the inferior olive from the mesencephalon and superior colliculus in the cat. An autoradiographic study. Exp Brain Res 45:333–348
Schonewille M, Luo C, Ruigrok TJ, Voogd J, Schmolesky MT, Rutteman M, Hoebeek FE, De Jeu MT, De Zeeuw CI (2006) Zonal organization of the mouse flocculus: physiology, input, and output. J Comp Neurol 497:670–682
Scott TG (1964) A unique pattern of localization within the cerebellum of the mouse. J Comp Neurol 22:1–8
Shook BL, Schlag-Rey M, Schlag J (1990) Primate supplementary eye field: I. Comparative aspects of mesencephalic and pontine connections. J Comp Neurol 301:618–642
Sillitoe RV, Marzban H, Larouche M, Zahedi S, Affanni J, Hawkes R (2005) Conservation of the architecture of the anterior lobe vermis of the cerebellum across mammalian species. Prog Brain Res 148:283–297
Stanton GB (1980a) Afferents to oculomotor nuclei from area "Y" in *Macaca mulatta*: an antegrade degeneration study. J Comp Neurol 192:377–385
Stanton GB (1980b) Topographical organization of ascending cerebellar projections from the dentate and interposed nuclei in *Macaca mulatta*: an anterograde degeneration study. J Comp Neurol 190:699–731
Steiger HJ, Büttner-Ennever JA (1979) Oculomotor nucleus afferents in the monkey demonstrated with horseradish peroxidase. Brain Res 160:1–15
Stilling B (1843) Ueber die Textur und Function der Medulla oblongata. F.Enke, Erlangen
Stilling B (1864) Untersuchungen über den Bau des kleinen Gehirns des Menschen. Fischer, Cassel
Strick PL, Dum RP, Fiez JA (2009) Cerebellum and nonmotor function. Annu Rev Neurosci 32:413–434
Strominger NL, Truscott TC, Miller RA, Royce GJ (1979) An autoradiographic study of the rubroolivary tract in the rhesus monkey. J Comp Neurol 183:33–45
Sugihara I, Quy PN (2007) Identification of aldolase C compartments in the mouse cerebellar cortex by olivocerebellar labeling. J Comp Neurol 500:1076–1092
Sugihara I, Shinoda Y (2004) Molecular, topographic, and functional organization of the cerebellar cortex: a study with combined aldolase C and olivocerebellar labeling. J Neurosci 24:8771–8785
Sugihara I, Shinoda Y (2007) Molecular, topographic, and functional organization of the cerebellar nuclei: analysis by three-dimensional mapping of the olivonuclear projection and aldolase C labeling. J Neurosci 27(36):9696–9710
Sugihara I, Ebata S, Shinoda Y (2004) Functional compartmentalization in the flocculus and the ventral dentate and dorsal group y nuclei: an analysis of single olivocerebellar axonal morphology. J Comp Neurol 470:113–133
Sugihara I, Fujita H, Na J, Quy PN, Li BY, Ikeda D (2009) Projection of reconstructed single Purkinje cell axons in relation to the cortical and nuclear aldolase C compartments of the rat cerebellum. J Comp Neurol 512:282–304
Sugimoto T, Mizuno N, Uchida K (1982) Distribution of cerebellar fiber terminals in the midbrain visuomotor areas: an autoradiographic study in the cat. Brain Res 238:353–370
Swenson RS, Castro AJ (1983a) The afferent connections of the inferior olivary complex in rats. An anterograde study using autoradiographic and axonal degeneration techniques. Neuroscience 8:259–275
Swenson RS, Castro AJ (1983b) The afferent connections of the inferior olivary complex in rats: a study using the retrograde transport of horseradish peroxidase. Am J Anat 166:329–341
Tan J, Epema AH, Voogd J (1995a) Zonal organization of the flocculovestibular nucleus projection in the rabbit: a combined axonal tracing and acetylcholinesterase histochemical study. J Comp Neurol 356:51–71

Tan J, Gerrits NM, Nanhoe R, Simpson JI, Voogd J (1995b) Zonal organization of the climbing fiber projection to the flocculus and nodulus of the rabbit: a combined axonal tracing and acetylcholinesterase histochemical study. J Comp Neurol 356:23–50

Tan J, Simpson JI, Voogd J (1995c) Anatomical compartments in the white matter of the rabbit flocculus. J Comp Neurol 356:1–22

Teune TM, van der Burg J, van der Moer J, Voogd J, Ruigrok TJH (2000) Topography of cerebellar nuclear projections to the brain stem in the rat. In: Gerrits NM, Ruigrok TJH, De Zeeuw CI (eds) Cerebellar modules: molecules, morphology and function, vol 124. Progr Brain Res Elsevier Science B.V., Amsterdam, pp 141–172

Thomas A (1897) Le cervelet: étude anatomique, clinique et physiologique. G. Steinheil, Paris

Tian JR, Lynch JC (1997) Subcortical input to the smooth and saccadic eye movement subregions of the frontal eye field in cebus monkey. J Neurosci 17:9233–9247

Tokuno H, Takada M, Nambu A, Inase M (1995) Somatotopical projections from the supplementary motor area to the red nucleus in the macaque monkey. Exp Brain Res 106:351–355

Tolbert DL, Massopust LC, Murphy MG, Young PA (1976) The anatomical organization of the cerebello-olivary projection in the cat. J Comp Neurol 170:525–544

Trott JR, Armstrong DM (1987) The cerebellar corticonuclear projection from lobule Vb/c of the cat anterior lobe: a combined electrophysiological and autoradiographic study. Exp Brain Res 68:339–354

Trott JR, Apps R, Armstrong DM (1998) Zonal organization of cortico-nuclear and nucleo-cortical projections of the paramedian lobule of the cat cerebellum. 1 the C1 zone. Exp Brain Res 118:298–315

Uddenberg N (1968) Differential localization in dorsal funiculus of fibres originating from different receptors. Exp Brain Res 4:367–376

Uusisaari M, Knopfel T (2010) GlyT2+ neurons in the lateral cerebellar nucleus. Cerebellum 9:42–55

Van Ham JJ, Yeo CH (1992) Somatosensory trigeminal projections to the inferior olive, cerebellum and other precerebellar nuclei in rabbits. Eur J Neurosci 4:302–317

van Kan PLE, Houk JC, Gibson AR (1993) Output organization of intermediate cerebellum of the monkey. J Neurophysiol 69:57–73

Verhaart WJC (1936) Die zentrale Haubenbahn bei Affen und Menschen. Schweiz Arch Neurol Psychiat 38:270–283

Verhaart WJ, Wieringen-Rauws GA (1950) On cerebro-cerebellar atrophy. Folia Psychiatr Neurol Neurochir Neerl 53:481–501

von Hartmann-Monakow KH, Akert K, Künzle H (1979) Projections of precentral and premotor cortex to the red nucleus and other midbrain areas in *Macaca fascicularis*. Exp Brain Res 34:91–105

Voogd J (1964) The cerebellum of the cat. Van Gorcum, Assen

Voogd J (1969) The importance of fiber connections in the comparative anatomy of the mammalian cerebellum. In: Llinas R (ed) Neurobiology of cerebellar evolution and development. AMA, Chicago, pp 493–514

Voogd J (2004) Cerebellum and precerebellar nuclei. In: Paxinos G, Mai JK (eds) The human nervous system. Elsevier, Amsterdam, pp 322–392

Voogd J, Barmack NH (2006) Oculomotor cerebellum. Prog Brain Res 151:231–268

Voogd J, Bigaré F (1980) Topographical distribution of olivary and cortico-nuclear fibres in the cerebellum: a review. In: Courville J (ed) The olivary nucleus. Anatomy and physiology. Raven, New York, pp 207–234

Voogd J, Ruigrok TJ (2004) The organization of the corticonuclear and olivocerebellar climbing fiber projections to the rat cerebellar vermis: the congruence of projection zones and the zebrin pattern. J Neurocytol 33:5–21

Voogd J, Gerrits NM, Hess DT (1987a) Parasagittal zonation of the cerebellum in macaques: an analysis based on acetylcholinesterase histochemistry. In: Glickstein M, Yeo C, Stein J (eds) Cerebellum and neuronal plasticity. Plenum Press, London, pp 15–39

Voogd J, Hess DT, Marani E (1987b) The parasagittal zonation of the cerebellar cortex in cat and monkey. Topography, distribution of acetylcholinesterase and development. In: King JS (ed) New concepts in cerebellar neurobiology. Liss, New York, pp 183–220

Voogd J, Gerrits NM, Ruigrok TJ (1996) Organization of the vestibulocerebellum. Ann NY Acad Sci 781:553–579

Voogd J, Pardoe J, Ruigrok TJ, Apps R (2003) The distribution of climbing and mossy fiber collateral branches from the copula pyramidis and the paramedian lobule: congruence of climbing fiber cortical zones and the pattern of zebrin banding within the rat cerebellum. J Neurosci 23:4645–4656

Voogd J, Schraa-Tam CK, van der Geest JN, De Zeeuw CI (2011) Visuomotor cerebellum in human and nonhuman primates. Cerebellum. doi:10.1007/s12311-010-0204-7

Walberg F (1982) The trigemino-olivary projection in the cat as studied with retrograde transport of horseradish peroxidase. Exp Brain Res 45:101–107

Weber JT, Partlow GD, Harting JK (1978) The projection of the superior colliculus upon the inferior olivary complex of the cat: an autoradiographic and horseradish peroxidase study. Brain Res 144:369–377

Weidenreich F (1899) Zur Anatomie der zentralen Kleinhirnkerne der Säuger. Z Morphol Anthropol 1:259–312

Whitworth RH Jr, Haines DE (1983) The inferior olive of a prosimian primate *Galago senegalensis*. I. Conformation and spino-olivary projections. J Comp Neurol 219:215–227

Whitworth RH Jr, Haines DE (1986a) The inferior olive of Saimiri sciureus: olivocerebellar projections to the anterior lobe. Brain Res 372:55–71

Whitworth RH Jr, Haines DE (1986b) On the question of nomenclature of homologous subdivisions of the inferior olivary complex. Arch Ital Biol 124:271–317

Wiberg M, Blomqvist A (1984a) The projection to the mesencephalon from the dorsal column nuclei. An anatomical study in the cat. Brain Res 311:225–244

Wiberg M, Blomqvist A (1984b) The spinomesencephalic tract in the cat: its cells of origin and termination pattern as demonstrated by the intraaxonal transport method. Brain Res 291:1–18

Wiberg M, Westman J, Blomqvist A (1986) The projection to the mesencephalon from the sensory trigeminal nuclei. An anatomical study in the cat. Brain Res 399:51–68

Wiberg M, Westman J, Blomqvist A (1987) Somatosensory projection to the mesencephalon: an anatomical study in the monkey. J Comp Neurol 264:92–117

Wiesendanger R, Wiesendanger M (1985) Cerebello-cortical linkage in the monkey as revealed by transcellular labeling with the lectin wheat germ agglutinin conjugated to the marker horseradish peroxidase. Exp Brain Res 59:105–117

Wylie DR, De Zeeuw CI, DiGiorgi PL, Simpson JI (1994) Projections of individual Purkinje cells of identified zones in the ventral nodulus to the vestibular and cerebellar nuclei in the rabbit. J Comp Neurol 349:448–463

Xiong G, Nagao S (2002) The lobulus petrosus of the paraflocculus relays cortical visual inputs to the posterior interposed and lateral cerebellar nuclei: an anterograde and retrograde tracing study in the monkey. Exp Brain Res 147:252–263

Yamamoto M (1978) Localization of rabbit's flocculus Purkinje cells projecting to cerebellar lateral nucleus and the nucleus prepositus hypoglossi investigated by means of the horseradish peroxidase retrograde transport. Neurosci Lett 7:197–202

Yamamoto M (1979) Topographical representation in rabbit flocculus for various afferent inputs from the brain stem investigated by means of retrograde transport of horseradish peroxidase. Neurosci Lett 12:29–34

Yamamoto F, Sato Y, Kawasaki T (1986) The neuronal pathway from the flocculus to the oculomotor nucleus: an electrophysiological study of group y neurons in cats. Brain Res 371:350–354